Department of Communications and Networking

Interference control and radio spectrum allocation in shared spectrum access

Byungjin Cho

Aalto University

DOCTORAL DISSERTATIONS

Aalto University publication series
DOCTORAL DISSERTATIONS 125/2016

Interference control and radio spectrum allocation in shared spectrum access

Byungjin Cho

A doctoral dissertation completed for the degree of Doctor of Science (Technology) to be defended, with the permission of the Aalto University School of Electrical Engineering, at a public examination held at the lecture hall T2 of the school on 5 August 2016 at 12.

Aalto University
School of Electrical Engineering
Department of Communications and Networking

Supervising professor
Prof. Riku Jäntti, Aalto University, Finland

Thesis advisor
Prof. Riku Jäntti, Aalto University, Finland

Preliminary examiners
Prof. Viktoria Fodor, KTH Royal Institute of Technology, Sweden
Prof. Marina Petrova, RWTH Aachen University, Germany

Opponent
Prof. Miao Pan, University of Houston, USA

Aalto University publication series
DOCTORAL DISSERTATIONS 125/2016

ISBN 978-952-60-6887-9 (printed)
ISBN 978-952-60-6888-6 (pdf)
ISSN-L 1799-4934
ISSN 1799-4934 (printed)
ISSN 1799-4942 (pdf)
http://urn.fi/URN:ISBN:978-952-60-6888-6

Unigrafia Oy
Helsinki 2016

Finland

441 697
Printed matter

Aalto University

Abstract

Aalto University, P.O. Box 11000, FI-00076 Aalto www.aalto.fi

Author
Byungjin Cho

Name of the doctoral dissertation
Interference control and radio spectrum allocation in shared spectrum access

Publisher School of Electrical Engineering

Unit Department of Communications and Networking

Series Aalto University publication series DOCTORAL DISSERTATIONS 125/2016

Field of research Communication Engineering

Manuscript submitted 17 February 2016 **Date of the defence** 5 August 2016

Permission to publish granted (date) 24 May 2016 **Language** English

☐ **Monograph** ☒ **Article dissertation** ☐ **Essay dissertation**

Abstract

With demands on the radio spectrum intensifying, it is necessary to use this scarce resource as efficiently as possible. One way forward is to apply flexible authorization schemes such as shared spectrum access. While such schemes are expected to make additional radio resource available and lower the spectrum access barriers, they also bring new challenges toward effectively dealing with the created extra interference which degrades the performance of networks, limiting the potential gains in a shared use of spectrum. In this thesis, to address the interference issue, different spectrum access schemes and deployment scenarios are investigated.

Firstly, we consider licensed shared access where database-assisted TV white space network architecture is employed to facilitate the controlled access of the secondary system to the TV band. The operation of the secondary system is allowed only if the quality of service experienced by the incumbent users is preserved. Furthermore, the secondary system should benefit itself from utilizing the TV band in licensed shared access mode. One challenge for efficient operation of the licensed secondary system is to control the cross-tier interference generated at the TV receiver, taking into account the self-interference in the secondary system.

Secondly, we consider co-primary shared access where multiple operators share a part of their spectrum. This can be done in two different operational levels, users and cells. The user level is done in the context of D2D communications where two users subscribed to different operators can transmit directly to each other. The cell level allows spectrum sharing between two small cells, e.g., indoor and outdoor small cells, in a dense urban environments. The main challenges for such scenarios are to manage the cross-tier interference generated by other users or cells subscribed to different operators, and to identify the amount of radio spectrum each operator contributes.

There are several approaches to reduce the risk of interference, but they often come at a high price in terms of complexity and signaling overhead. In this thesis, we aim to propose low complexity mechanisms that take interference control and radio spectrum allocation into account. The proposed mechanisms are based on tractable models which characterize the effects of the fundamental design parameters on the system behavior in shared spectrum access. The models are leveraged to capture the statistic of the aggregate interference and its effects on the performance metrics.

Keywords Flexible spectrum use, interference models, stochastic geometry, game theory

ISBN (printed) 978-952-60-6887-9 **ISBN (pdf)** 978-952-60-6888-6

ISSN-L 1799-4934 **ISSN (printed)** 1799-4934 **ISSN (pdf)** 1799-4942

Location of publisher Helsinki **Location of printing** Helsinki **Year** 2016

Pages 158 **urn** http://urn.fi/URN:ISBN:978-952-60-6888-6

Preface

The research work towards this doctoral thesis has been carried out at the Department of Communications and Networking at Aalto University School of Electrical Engineering during the years 2011-2015. The work has been funded by the TEKES project IMANET+, the Academy of Finaland project SMACIW, and the EU FP7 project METIS. This thesis is the result of encouragements, inspirations, education and all the helps that I have received during years of study from professors, colleagues, friends and family.

First and foremost, I would like to express my sincere gratitude to my supervisor, Professor Riku Jäntti, for his guidance, constructive criticism and encouragement during these years. His suggestions have helped generalizing our findings thereby opening new directions to our research work. I would also like to thank him for generating a pleasant and secure working environment.

I am deeply grateful to Dr. Konstantinos Koufos for his countless advices and feedbacks, and for his patience and consideration in advising my study. I would also like to extend my gratitude to my co-authors: Dr. Zexian Li and Dr. Mikko A. Uusitalo from Nokia Research Center, Dr. Kalle Ruttik from Aalto University and Prof. Seong-Lyun Kim from Yeonsei University. Their sharp comments and technical help enabled me to finalize the publications. I am deeply indebted to all of you.

My warm thanks also go to the thesis pre-examiners, Prof. Viktoria Fodor from KTH Royal Institute of Technology, and Prof. Marina Petrova from RWTH Aachen University, for their constructive comments that helped improving the clarity and the presentation quality of the thesis. I would also like to thank Prof. Miao Pan from University of Houston for accepting to be the opponent in the public defense of this thesis.

I would like to thank the current and former Comnet members: Dr.

Aftab Hossain, Dr. Aamir Mahmood, Dr. Duan Ruifeng, Mr. Jussi Kerttula, Lic.Sc. Turo Halinen, and Dr. Zhong Zheng for helpful discussions both on academic and non-academic matters. The Comnet secretaries and supporting team are also acknowledged for making our everyday life easier. Thanks also go to my friends for making my life colorful.

I would like to thank my parents and parents-in-law deeply for their careful consideration, and the many years of patience and dedication during my studies that provided soul foundation for this work. Lastly but certainly not least, my sincerest appreciation and love go to my wife, Suji Lim, life companion and best friend - emotionally and intimately. Her encouragement, love and existence itself have kept me mostly sane and made my hardest days less hard throughout my doctoral years.

Helsinki, July 7, 2016,

Byungjin Cho

Contents

List of Publications

This thesis consists of an overview and of the following publications which are referred to in the text by their Roman numerals.

I B. Cho, K. Koufos, K. Ruttik, and R. Jäntti. Power allocation in the TV white space under constraint on secondary system self-interference. *Journal of Electrical and Computer Engineering*, vol. 2012, June 2012.

II B. Cho, K. Koufos, and R. Jäntti. Interference control in cognitive wireless networks by tuning the carrier sensing threshold. In *Proc. IEEE International Conference on Cognitive Radio Oriented Wireless Networks (CROWNCOM)*, pp. 185-189, June 2013.

III B. Cho, K. Koufos, and R. Jäntti. Bounding the mean interference in matérn type II hard-core wireless networks. *IEEE Wireless Communications Letters*, vol. 2, no. 5, pp. 563-566, October 2013.

IV B. Cho, K. Koufos, and R. Jäntti. Spectrum allocation and mode selection for overlay D2D using carrier sensing threshold. In *Proc. IEEE International Conference on Cognitive Radio Oriented Wireless Networks (CROWNCOM)*, pp. 26-31, June 2014.

V B. Cho, K. Koufos, R. Jäntti, Z. Li, and M. A. Uusitalo. Spectrum allocation for multi-operator Device-to-Device communication. In *Proc. IEEE International Conference on Communications (ICC)*, pp. 5454-5459, June 2015.

VI B. Cho, K. Koufos, R. Jäntti, and S.-L, Kim. Co-primary spectrum sharing for inter-operator Device-to-Device communication. *IEEE Journal of Selected Area in Communications (JSAC)*, submitted on 30th, April 2016.

VII B. Cho, K. Koufos, K. Ruttik, and R. Jäntti. Modeling the interference generated from car base stations towards indoor femto-cells. In *Proc. International Federation of Automatic control (IFAC) Symposium on Telematics Applications*, pp. 96-101, November 2013.

Author's Contribution

Publication I: "Power allocation in the TV white space under constraint on secondary system self-interference"

The author carried out the theoretical analysis and generated the results. Dr Konstantinos Koufos formulated the problem and proposed the power allocation scheme. The author, together with Dr Konstantinos Koufos, wrote the paper under the guidance of Dr Kalle Ruttik and Professor Riku Jäntti.

Publication II: "Interference control in cognitive wireless networks by tuning the carrier sensing threshold"

The author formulated the problem, carried out the theoretical analysis and generated the results. The author, together with Dr Konstantinos Koufos, validated the proposed models and wrote the paper together under the supervision of Professor Riku Jäntti.

Publication III: "Bounding the mean interference in matérn type II hard-core wireless networks"

The author proposed models for tight bounds for the mean interference in contention-based networks, carried out the theoretical analysis and generated the results. The author, together with Dr Konstantinos Koufos, validated the proposed models and wrote the paper together under the supervision of Professor Riku Jäntti.

Publication IV: "Spectrum allocation and mode selection for overlay D2D using carrier sensing threshold"

The author formulated the problem, carried out the theoretical analysis and generated the results. The author, together with Dr Konstantinos Koufos, validated the proposed models and wrote the paper together under the supervision of Professor Riku Jäntti.

Publication V: "Spectrum allocation for multi-operator Device-to-Device communication"

The author formulated the problem, carried out the theoretical analysis and generated the results. The author, together with Dr Konstantinos Koufos, validated the proposed models and wrote the paper together under the supervision of Professor Riku Jäntti, Dr Zexian Li, and Dr Mikko A. Uusitalo.

Publication VI: "Co-primary spectrum sharing for inter-operator Device-to-Device communication"

The author formulated the problem, carried out the theoretical analysis and generated the results. The author, together with Dr Konstantinos Koufos, validated the proposed models and wrote the paper together under the supervision of Professors Riku Jäntti and Seong-Lyun Kim.

Publication VII: "Modeling the interference generated from car base stations towards indoor femto-cells"

Professor Riku Jäntti formulated the problem. The author carried out the theoretical analysis and generated the results. The author, together with Dr Konstantinos Koufos, validated the proposed models and wrote the paper together under the supervision of Dr Kalle Ruttik and Professor Riku Jäntti.

List of Abbreviations

ASA	Authorized Shared Access
BPP	Binomial Point Process
BS	Base Station
CCA	Clear Channel Assessment
CDF	Cumulative Distribution Function
CF	Characteristic Function
CS	Carrier Sensing
CSA	Co-primary Shared Access
CSI	Channel State Information
CSMA	Carrier Sensing Multiple Access
D2D	Device-to-Device
ECC	Electronic Communications Committee
ED	Energy Detection
FCC	Federal Communications Commission
FW	Fenton-Wilkinson
HCD	Hardcore Distance
ISM	Industrial, Scientific, and Medical
LSA	Licensed Shared Access
LT	Laplace Transform
MAC	Medium Access Control

MC	Monte Carlo
MGF	Moment Generation Function
MNO	Mobile Network Operator
MPP	Matérn-hardcore Point Process
NE	Nash Equilibrium
OFCOM	Federal Office of Communications
P2P	Peer-to-Peer
PCF	Pair Correlation Function
PDF	Probability Density Function
PF	Proportional Fair
PGFL	Probability Generating Functional
PPP	Poisson Point Process
QoS	Quality of Service
RNC	Radio Network Controller
RV	Random Variable
SINR	Signal-to-Interference-plus-Noise Ratio
SIR	Signal-to-Interference Ratio
SSI	Simple Sequential Inhibition
SY	Schwarz-Yeh
TVWS	TV White Space
UMi	Urban Micro
UHF	Ultra High Frequency
V2V	Vehicle-to-Vehicle

List of Symbols

Greek Symbols

α	Pathloss exponent
β_i	Spectrum fraction in inter-operator D2D mode of operator i
β_i^c	Spectrum fraction in cellular mode of operator i
β_i^d	Spectrum fraction in intra-operator D2D mode of operator i
γ	SINR
γ_n	Normalized SIR
γ_t	SINR target
$\gamma_{k,p}$	SINR at the p-th test point of k-th secondary cellular BS
$\Gamma(\cdot)$	Gamma function
δ	Hardcore distance
$\zeta(\cdot)$	Riemann zeta function
η	Car isolation
κ	Probability that a BS is active
λ	Density of nodes
λ_2	User density in area S_2
λ_p	Density of PPP
λ_m	Density of MPP
λ_i^b	Density of BSs in operator i

λ_i^c	Density of cellular users in operator i
λ_i^d	Density of intra-operator D2D users in operator i
λ_j^{vu}	Density of vehicles on j-th vertical street
$\lambda_{j'}^{vu}$	Density of vehicles on j'-th horizontal street
μ_i	Intra-D2D user target rate of operator i
μ_w	Mean of w
μ_z	Mean of z
ξ	Scaling constant equal to $10/\log(10)$
σ_w	Standard deviation of w
σ_z	Standard deviation of z
τ_i	Cellular user target rate of operator i
Φ	Set of nodes
Φ^{SU}	Set of nodes in TVWS
Φ_i^{CM}	Set of users in cellular uplink mode of operator i
$\Phi_i^{CM,a}$	Set of users in cellular mode of operator i
Φ_i^{DM}	Set of users in intra-operator D2D mode of operator i
$\Phi_i^{DM'}$	Set of users in inter-operator D2D mode of operator i
Φ_j^{VU}	Set of vehicles on j-th vertical street
$\Phi_{j'}^{VU}$	Set of vehicles on j'-th horizontal street

Latin Symbols

$A(r)$	Intersection area of two circles whose centers are at distance r
$f_\gamma(t)$	PDF of γ
$F_\gamma(\gamma_t)$	CDF of γ at γ_t
$g_{m,\theta}$	Gamma distributed with scale m and shape θ
$g(r)$	PCF at distance r

I	Aggregate interference
$I_{\triangle}$	Interference margin
$I_{\triangle_l}$	Lower bound of interference margin
$I_{\triangle_l}^{su}$	Interference margin at secondary test points
I_b	Interference from a BPP
I_p	Interference from a PPP
I^{SU}	Interference at a TV receiver generated from Φ^{SU}
I_i^{CM}	Interference at a BS generated from Φ_i^{CM}
I_i^{DM}	Interference at a D2D receiver generated from Φ_i^{DM}
$I_i^{DM'}$	Interference at a D2D receiver generated from $\Phi_i^{DM'}$
$I_{i,tx}^{DM}$	Interference at a D2D transmitter generated from Φ_i^{DM}
$I_{i,tx}^{DM'}$	Interference at a D2D transmitter generated from $\Phi_i^{DM'}$
I_j^{VU}	Interference at a femtocell receiver generated from Φ_j^{VU}
$I_{j'}^{VU}$	Interference at a femtocell receiver generated from $\Phi_{j'}^{VU}$
I_{IN}	Sum of aggregate interference and noise power
k	Number of transmitters
K	Number of co-primary operators
K_c	Number of secondary cellular transmitters
l_k	Distance-based propagation pathloss from k-th transmitter
L_k	Propagation pathloss including fading from k-th transmitter
$\mathcal{L}_I(\cdot)$	LT of I
N	Noise power
O_t	Outage probability target
${}_pF_q(\cdot)$	Generalized hypergeometric function for integer p and q
P	Transmit power level
P_d	Transmit power density

P_k	Transmit power level from k-th transmitter
q_i^d	Probability of a D2D user in i-th intra-operator D2D mode
q	Probability of a D2D user in inter-operator D2D mode
Q_i^c	Cellular user rate of i-th operator
Q_i^d	Intra-operator D2D user rate of operator i
Q_i^s	Inter-operator D2D user rate of operator i
$Q^{-1}(\cdot)$	Inverse of the Gaussian $Q(\cdot)$ function
r_c	Distance between a cellular user and its nearest BS
r_d	Pairwise distance of a D2D pair
r_k	Distance between a receiver and k-th transmitter
$r_{k,t}$	Distance between a transmitter and k-th transmitter
r_n	TV protection area radius
r_{TV}	TV service area radius
R	Average spectral efficiency
R_i^c	Cellular uplink spectral efficiency of operator i
R_i^d	Intra-operator D2D link spectral efficiency of operator i
R_i^s	Inter-operator D2D link spectral efficiency of operator i
$\mathcal{R}^n$	n-dimensional real space
S	Secondary deployment area
S_f	Transmitter's footprint
S_1	Secondary deployment area, $r_{TV} + r_n + \delta \leq r$
S_2	Secondary deployment area, $r_{TV} + r_n \leq r < r_{TV} + r_n + \delta$
U_i	Utility of i-th operator
v_k	Activity indication from k-th transmitter
w	Lognormal RV of W
$\mathcal{W}(\cdot)$	Lambert function

$\mathcal{W}_0(\cdot)$	Principal branch of Lambert function
W	Useful signal power level
$\overline{W}$	Mean useful signal power level
x	RV modeling fading
x_z	Gaussian RV with zero mean and σ_z
x_w	Gaussian RV with zero mean and σ_w
z	Lognormal RV of I_{IN}

1. Introduction

1.1 Motivation

Increasing demand for mobile data services has pushed a major change in the philosophy of radio spectrum management. Traditionally, the allocation of spectrum has been static in the sense that spectrum regulation agencies usually confine services to a fixed spectrum band and grant exclusive access to a license holder. In the past, this static spectrum allocation has worked effectively for protecting the licensee from harmful radio interference. However, licensed access prohibits the usage of the spectrum when it is underutilized or not even used at all. The inflexibility of exclusive usage leads to inefficient spectrum utilization [1,2].

To enable flexibility and increased utilization, the concept of shared use of spectrum has been introduced. *The shared use of spectrum allows multiple nodes to access the same range of frequencies under certain conditions* [3]. This concept is exemplified by shared use of unlicensed spectrum in Industrial, Scientific, and Medical (ISM) bands. In ISM bands, multiple potential nodes such as medical and sensor devices and all WLAN users access the spectrum without external regulations. Although, such unregulated access significantly lowers the market entry barriers, it produces uncontrolled interference and consequently makes it challenging to guarantee any Quality of Service (QoS). An alternative solution, which can potentially solve this dilemma, is a shared use of the licensed spectrum based on flexible regulatory regimes. For instance, coexisting nodes may operate across various licensed bands with different authorization modes.

Authorized Shared Access (ASA)/Licensed Shared Access (LSA) is a licensed spectrum sharing paradigm [4] where a primary license holder (incumbent) would grant spectrum access rights to one or more secondary

nodes in LSA mode (LSA licensees). A key benefit of the LSA concept is to guarantee a certain level of spectrum access and protection against harmful interference for both incumbent and licensees that operate different services subject to different conditions. The LSA concept is based on the geolocation database called the LSA repository which contains information on spectrum availability and associated conditions. The LSA is mainly driven by European regulators [5, 6] on gaining access to 2.3 - 2.4 GHz and possibly 3.4 - 3.8 GHz spectrum for mobile broadband. In Finland, the LSA concept has been successfully trialed with a LTE network in the 2.3 GHz shared band in April 2013 [7].

LSA in TV White Space (TVWS) has also been promoted by using a geolocation-based licensing approach [8–12]. In the context of the LSA, secondary spectrum access in the TV band can be performed in a more controlled manner with database-assisted TVWS network architecture, compared to unregulated access. Therein, licensed secondary systems, e.g., infrastructure-based systems or ad-hoc type systems, can obtain the available TV channel information by querying a geolocation database instead of sensing the local spectrum environment as in traditional dynamic spectrum sharing systems. Such an approach enables a certain QoS for the secondary system as in LSA mode with some operational conditions, protecting the incumbent and offering the necessary possibilities to the LSA licensees.

Co-primary Shared Access (CSA) is another concept designed to enable spectrum sharing, where primary license holders jointly use a part (or the whole) of their licensed spectrum to enable an operator to cope with temporary peaks in capacity demand [10]. Mutual interference can be minimized by the use of joint databases which are co-operatively settled between the co-primary partners. Potential scenarios of CSA include Peer-to-Peer (P2P) communication, e.g., Device-to-Device (D2D) or Vehicle-to-Vehicle (V2V) communication, and small-cell deployments, e.g., femtocells, picocells, and microcells, [13, 14]. These scenarios have low transmission powers and, consequently, interference between cells or between users is typically low, thus allowing the reuse of the same chunk of spectrum in proximity based direct communication or among neighboring buildings. To guarantee efficient spectrum sharing, the exchange of information among participating operators in a competitive environment is inevitable [14]. Therefore, to realize the benefits of CSA, operators need to manage the market values in order to strike a balance between cooper-

ation and competition.

One of the main technological challenges in any shared use of spectrum is to design radio resource management efficiently in order to maximize the spectrum usage efficiency. Efficient radio resource management algorithms are heavily tied to information gathering and processing. The corresponding solutions may require lots of resources that might not be available, or may be very costly and complex to implement. Therefore, the optimal decisions always have high dependencies on the overhead and scalability. For this reason, it is hoped that the research conducted in this thesis will shed more light on efficient use of shared spectrum for future networks with low overhead and low complexity.

1.2 Scope

A fundamental issue in sharing the use of spectrum is to assess the impact of two or more technologies on each other when operating on the same frequency band or on adjacent bands. Interference is the main performance limiting parameter in a shared frequency band, due to the nature of the wireless medium. There are two types of interference: cross-tier interference and intra-tier interference (self-interference). The tiers are either different systems or different operators. Cross-tier interference is the interference experienced by a node in a tier from nodes in another tier, that is, interference generated at a node in the primary system from nodes in a secondary system, or interference generated to a node belonging to an operator from nodes belonging to different operator. On the contrary, intra-tier interference is the interference experienced by a node in the same tier.

For efficient spectrum sharing, interference coordination and avoidance are of primary interest. The objective of interference coordination is to limit interference to a level such that the performance at a receiver is deemed acceptable. The focus under this objective is on controlling the interference to a desired level through adjusting some transmission parameters. On the other hand, the objective of interference avoidance is to provide better interference immunity by avoiding the assignment of strongly interfering nodes to the same time/frequency resources, i.e., by resource partitioning and scheduling coordination approaches. The focus under this objective is on properly partitioning the radio spectrum so that the spectral efficiency is not reduced. For interference control and avoid-

ance in shared spectrum, some operational parameters can be adjusted by using some central entity or network element, e.g., geolocation database, LSA controller, or Radio Network Controller (RNC).

A basis for efficient interference control and radio spectrum allocation is the interference model which predicts whether a set of concurrent transmissions in the shared band may interfere with one another. Essentially efficient interference control and spectrum allocation are done at the expense of increased computational complexity and signaling overhead induced by information exchange among coexisting nodes. For instance, with only knowledge of the traffic load such as the total number of simultaneous transmissions in the shared band, a tractable interference model enables the estimation of the average channel quality at any random point in a coverage area and the design of the efficient spectrum management.

1.3 Objective and Content

The objective of this thesis is to promote efficient use of shared spectrum, devising low complex mechanisms that take interference control and radio spectrum allocation into account. The proposed mechanisms are based on the tractable models which characterize and better understand the effects of the fundamental design parameters on the system behavior in spectrum sharing. The models are leveraged to develop closed-form mathematical frameworks for performance metrics and capture statistics of the aggregate interference in different spectrum access schemes, technologies, and deployment scenarios. In this thesis, we focus on two types of shared spectrum access schemes. One considers to exploit the TV band in LSA mode, while another considers to utilize the cellular band in primary user mode. In addition, three technologies are considered with different deployment scenarios: (i) geolocation database-assisted secondary systems (LSA licensee) in TVWS deployment, (ii) direct communications between proximity users subscribed to different operators in random deployment, and (iii) moving networks [9] coexisting on the same spectrum with indoor femtocell networks in Manhattan street deployment.

This thesis is structured as follows. Chapter 2 introduces the commonalities in methodologies for performance metrics, and gives an overview of the modeling approaches for interference statistics.

Chapter 3 considers database-assisted secondary systems in TVWS, outlining the methods and results of Publication I and Publication II. The

aim of the methods is to control the interference generated by two different types of secondary systems in LSA mode. For infrastructure type systems, e.g., cellular systems, we suggest a low-complexity power allocation algorithm incorporating secondary self-interference constraint. For ad-hoc type systems, e.g., WLAN with the Carrier Sensing Multiple Access (CSMA)-type Medium Access Control (MAC), we suggest a low complexity Carrier Sensing (CS) threshold tuning algorithm in primary-secondary system setup. The methods enable the geolocation database to operate with low complexity algorithms in order to handle frequent spectrum access requests in real time.

Chapter 4 considers inter-operator D2D communication in the cellular band for CSA, outlining the methods and results of Publication IV, Publication V, and Publication VI. The aim of the methods is to handle mode selection and spectrum allocation for D2D communication. The mode selection involves controlling the interference, since it has a distributed nature eliminating communication signaling overhead between D2D users and their home BSs, based on the spectrum usage activity. The spectrum allocation algorithm enables the coordinated common usage of dedicated spectral resources by devices from different operators, taking into account individual intra-operator network load.

Chapter 5 considers outdoor moving networks coexisting with indoor small-cell networks for CSA, outlining the methods and results of Publication VII. The aim of the methods is to control the interference generated from the outdoor vehicles in microcell networks along urban streets to the indoor femtocell networks. The methods are based on a model for calculating the performance of the femtocell networks. The methods enable a dynamic evaluation of outage probability in coordination mechanisms between the involved co-primary small-cell networks and cross-tier interference control. Finally, conclusions and future research directions are discussed in Chapter 6.

1.4 Contribution

This thesis is composed of a summary and seven Publications. A brief overview of the contributions in each Publication is given in this section.

In Publications I and II, inter-system spectrum sharing between a TV system and a secondary system in LSA mode is considered. We suggest methods for controlling some operational parameters in a licensed sec-

ondary system. In Publication I, a cellular system is considered as a candidate for spectrum access in TVWS. To bound the maximum allowable mean interference generated at the TV receivers, we propose to allocate proper transmission power levels in the downlink of cellular systems in TVWS. The existing power allocation rules adopted by the ECC [15] and FCC [16] do not take into account self-interference in the secondary system when identifying the transmission power levels. Unlike the existing ECC and FCC rules, we present power allocation as an optimization problem under a constraint where self-interference in the cellular system is taken into account as in LSA mode. The results of this Publication are useful for cellular system planning in TVWS.

In Publication II, a WLAN system has been considered as another candidate for secondary spectrum access in TVWS. We propose to control the CS threshold in the licensed secondary wireless systems with a finite deployment area. The CS threshold can be used as a common parameter to control the density of active secondary users in wireless systems with contention control thereby enabling primary system protection and avoiding strong intra-tier interference at the secondary system. The set of active users in wireless systems with contention control is conventionally modeled by a repulsive point process, Matérn-hardcore Point Process (MPP) type II. A common practice for computing the cross-tier aggregate mean interference at an arbitrary point on the plane is to approximate the MPP type II by using an equi-dense Poisson Point Process (PPP). Due to the existence of borders and protection regions between the two systems, the mean interference from a MPP type II is higher than the mean interference from the equi-dense PPP. To overcome this issue, we use multi-tier PPPs to bound the mean interference. Given the set of active users, we identified the CS threshold by computing the self-interference at a secondary user. The proposed method guarantees the primary system protection, and due to its low complexity, allows the geolocation database to compute the CS threshold in real-time, thereby adapting to frequent changes in secondary user density.

In Publication III, we are interested in computing the mean interference at a specific location in the network; the location of a transmitter performing the Clear Channel Assessment (CCA) or the location of a receiver evaluating a target link performance. While the mean interference at an arbitrary location in the plane can be sufficiently described by the density of effective points in MPP type II, the calculation of the one at a

specific location in the network is non-trivial due to a complicated Pair Correlation Function (PCF). We present tight bounds for the mean interference in contention-based networks.

In Publication IV, inter-user spectrum sharing among potential D2D users subscribed to same operator is considered. The first problem deals with a crowded communication environment where the participation of a Base Station (BS) to make a scheduling decision for cellular and D2D users causes large signaling overhead. We propose a mechanism to allocate spectrum for in-band overlay D2D communication. In the overlay approach, there is no cross-tier interference issue arising in the underlay approach. However, the cellular spectrum might be used inefficiently, if fixed spectrum is used without taking into account the activity of D2D. We use distributed mode selection algorithms where a potential D2D user measures the activity over the spectrum allocated for D2D transmissions and uses a CS threshold to decide about its transmission mode. Based on this method, we find spectrum allocation factors and CS thresholds for maximizing the rate of D2D users under the target rate constraint for cellular users. The results of this Publication can be useful for in-band D2D spectrum sharing in dense deployments, because a threshold-based test deciding their modes in a distributed way leads to less signaling overhead between D2D users and BSs.

In Publications V and VI, inter-operator spectrum sharing between different users subscribed to different operators is considered. We study how to share the spectrum among co-primary users for inter-operator D2D communication based on game theory, and how much spectrum each operator should commit for the spectrum sharing between two operators in Publication V, and among more than two operators in Publication VI. The results of these Publications propose some conditions guaranteeing the existence and stability of a unique equilibrium point, and show that operators experience significant performance gains as compared to the scheme without co-primary spectrum sharing.

In Publication VII, spectrum sharing between femtocell and microcell networks is considered. We study how to allocate operating parameters to the in-vehicle communication in microcell networks coexisting with indoor femtocell networks. We develop a model for aggregate interference distribution generated at indoor users from moving/parked vehicles in the Manhattan-grid. The proposed model is useful for assessing the outage probability for a given Signal-to-Interference Ratio (SIR) target at the

worst-case located femtocell due to cross-tier interference. The results of this Publication show how the density of vehicles, the uplink transmit power level and the vehicle isolation impact the outage probability at the femtocell. The observations are useful for frequency planning between street microcells and indoor femtocells.

2. Performance and interference characterizations

In this thesis, we focus on using a tractable approach to model the aggregate interference and characterize its effects on the performance metrics. For this purpose, in this chapter, we start by highlighting the commonalities in methodologies for performance metrics and in modeling approaches for the co-channel interference that are used in Chapters 3, 4 and 5.

Due to the shared nature of the wireless medium, the co-channel aggregate interference has a significant impact on the performance of wireless networks. The system performance can be characterized as a function of the random quantity, the Signal-to-Interference-plus-Noise Ratio (SINR) γ at a particular location given by

$$\gamma = \frac{W}{I + N} \tag{2.1}$$

where W is the received signal power, I is the aggregate interference, and N is the noise power. For satisfactory operation of wireless packet services, a target SINR γ_t must be satisfied at a certain outage probability target O_t. The signal reception is satisfactory if the following condition holds true

$$O_t \doteq \Pr[\gamma < \gamma_t] \doteq \int_0^{\gamma_t} f_\gamma(t)dt \doteq F_\gamma(\gamma_t) \tag{2.2}$$

where $f_\gamma(t)$ is the Probability Density Function (PDF) of the SINR γ and $F_\gamma(\gamma_t)$ is the Cumulative Distribution Function (CDF) of γ evaluated at γ_t. The distribution of the SINR plays an important role for system performance evaluation [17–19]. With a known expression for the distribution, the statistics of further performance metric, e.g., the outage probability and average rate, can be predicted, which otherwise should rely on complicated and time-consuming simulations. In order to evaluate the statistics of the SINR, we need a model for the useful signal distribution as well as for the interference distribution. In the following, we present

the performance characterization method used in this thesis. Afterwards the aggregate interference will be characterized with the spatial statistics of the interfering nodes.

2.1 Performance characterization method

In general, the PDF of the aggregate interference is unknown and it is typically characterized with Laplace Transform (LT), the Moment Generation Function (MGF), or the Characteristic Function (CF) of the PDF [17]. In this chapter, the LT is considered most relevant due to its suitability for Random Variables (RVs) with non-negative support, i.e., $\mathcal{L}_I(s) = E[e^{-sI}], I > 0$ and its moment generating properties, i.e., $E[I^n] = \lim_{s\to 0}(-1)^n \cdot \mathcal{L}_I^{(n)}(s)$. Naturally, the PDF of the aggregate interference can be obtained from the inverse transform of its LT. However, it is rather difficult to find the PDF in closed-form due to the complex nature of the LT expressions. In order to overcome the difficulty imposed by the non-existence of closed-form expressions for the PDF of the interference, some techniques have been used in the literature to utilize the LT and the moments of the aggregate interference as a basis for obtaining the distribution of SINR γ in (2.2). Thus further performance metrics can be evaluated [20].

In this section, we introduce some approaches including approximation and conversion methods. The former aims to find approximated expressions for interference distribution, and its LT. The latter aims to capture the outage probability by exploiting the LT or a few moments of the interference distribution based on the channel assumption which offers analytical tractability. Two channel environments are considered in this thesis, i) Nakagami-m (Rayleigh when $m = 1$) distributed fading for small-scale fading and ii) Lognormal distributed fading for large-scale fading.

2.1.1 Method #1. Approximated distribution

The distribution of aggregate interference can be approximated to a known distribution. The parameters of the approximated distribution are determined by setting appropriate moments which can be obtained from moment matching techniques [21]. For instance, if the PDF of the aggregate interference is approximated to a normal distribution or a gamma distribution by matching the first and second-order moments, the two parameters, the mean and the standard deviation of the normal distribution,

or the shape and the scale of the gamma distribution, can be found by setting the appropriate moments which are obtained from LT as in Publication VII and Chapter 5 of this thesis. When an interfering signal is modeled by a known RV, the distribution of the aggregate interference is modeled by the sum of the RVs. It is known that the LT of the distribution of the sum of independent RVs is the product of the LT of each RV [22].

Some distribution has no closed-form expression for the LT. For instance, there is no closed-form expression in defining the integral of the LT for the Lognormal distribution. Many methods have been proposed for approximating the sum of Lognormal RVs using another Lognormal RV, based on the two approaches: i) computing the parameters of the approximating distribution, e.g., the Fenton-Wilkinson (FW) method [23] or the Schwarz-Yeh (SY) method [24], and ii) approximating the LT integral, e.g., Gauss-Hermite integration in a conventional cellular network [25] or in a heterogeneous network [26]. In Publications I and II, the FW approximation has been adopted, since it is known to provide good approximations for the upper tails of the distribution and efficiently computed in closed-form making it suitable to use in numerical optimization [25, 27]. Also, only approximated expressions of LT are available for some spatial point process with the non-existence of the Probability Generating Functional (PGFL). In [28–31], the issue was addressed and approximated expressions for the LTs were derived. In Publications II, III, IV, V, and VI, we obtain the bounded expression using the PGFL of an independent point process, for a dependent point process.

2.1.2 Method #2. Nakagami-m fading assumption

By assuming Nakagami-m fading on the desired link, the exact distribution of the SINR can be obtained from accumulating the $\{0, 1, \cdots, (m-1)\}$-th derivatives of the LT of the aggregate interference evaluated at some value s, while the distribution for the aggregate interference cannot be obtained due to the non-existence of any closed-form expression for the PDF of the aggregate interference. The LT moments of the aggregate interference are essential to derive the exact distribution of the SINR and to quantify the outage (complement of coverage) probability, when Nakagami-m fading on the desired link is assumed. According to [32], the

outage probability is obtained as

$$O_t = 1 - e^{-sN} \sum_{n=0}^{m-1} \frac{(-s)^n}{n!} \frac{d^n}{ds^n} \mathcal{L}_I(s) \tag{2.3}$$

where $s = \gamma_t m/\overline{W}$ and $\overline{W}$ is the mean useful signal level. According to [33], the link spectral efficiency is derived in the same manner as follows

$$R = E[\ln(1+\gamma)] = \int_0^\infty \frac{\mathbf{Pr}\left[\gamma > \gamma_t\right]}{1+\gamma_t} d\gamma_t \tag{2.4}$$

This method is the most popular performance evaluation technique due to its simplicity and tractability, which is used in Chapters 4 and 5 of this thesis, and in Publications IV, V, VI, and VII. One challenge is how to obtain the LT of the aggregate interference. When the exact expression of the LT is unavailable, Method #1 in Section 2.1.1 can be used to find the approximation.

2.1.3 Method #3. Lognormal fading assumption

By assuming that a useful signal and a sum of the aggregate interference and noise power are modeled with a single Lognormal RV, respectively, the outage probability can be expressed in the form of a Gaussian Q-function, and can be derived with the first two moments of the Lognormal distribution.

Modeling the sum of the interfering signal and noise with a Lognormal RV can be expressed as $I_{IN} = I + N \sim 10^{z/10} = 10^{(\mu_z + x_z)/10}$ where μ_z (in dB) is the mean of z, x_z is a zero mean Gaussian random variable with standard deviation σ_z. The σ_z is interpreted as the slow-fading standard deviation of the interfering signal. Modeling the useful signal can be also expressed as in a similar manner $10^{(\mu_w + x_w)/10}$. By using the associated RVs, the outage probability can be expressed in Q-function [34, 35]

$$O_t = \mathbf{Pr}\left[10^{\frac{\mu_w + x_w}{10}} < \gamma_t 10^{\frac{\mu_z + x_z}{10}}\right] \tag{2.5a}$$

$$= 1 - Q\left(\frac{10\log_{10}(\gamma_t) - \mu_w + \mu_z}{\sqrt{\sigma_w^2 + \sigma_z^2}}\right) \tag{2.5b}$$

where $Q(\cdot)$ is the Gaussian Q-function, $\sigma_w^2 + \sigma_z^2$ denotes the variance of the RV $x_w - x_z$. By inverting equation (2.5b), the first moment of z can be expressed as

$$\mu_z = \sqrt{\sigma_w^2 + \sigma_z^2} \cdot Q^{-1}(1 - O_t) - 10\log_{10}(\gamma_t) + \mu_w \tag{2.6}$$

The FW method allows us to select the first two moments of z to match the moments of I_{IN}. Matching the moments of I_{IN} to the moments of z gives [36]

$$\mu_z = \xi \ln(E[I_{IN}]) - \sigma_z^2/2\xi \tag{2.7a}$$

$$\sigma_z^2 = \xi^2 \ln\left(1 + Var[I_{IN}]/E[I_{IN}]^2\right) \tag{2.7b}$$

From equations (2.6) and (2.7a), one turns the chance type of constraint (2.5) into the following interference constraint

$$E[I] \leq e^{\frac{1}{\xi}\left(\mu_z + \frac{\sigma_z^2}{2\xi}\right)} - N \doteq I_{\triangle} \tag{2.8a}$$

$$\leq e^{\frac{1}{\xi}\left(\sqrt{\sigma_w^2+\sigma_z^2}\cdot Q^{-1}(1-O_t) - 10\log_{10}(\gamma_t) + \mu_w + \frac{\sigma_z^2}{2\xi}\right)} - N \tag{2.8b}$$

where $I_{\triangle}$ is the interference margin describing the amount of permitted generated interference at the receiver. And the constraint in equation (2.8) can be evaluated by computing the the moments of I_{IN}, $E[I_{IN}]$ and $Var[I_{IN}]$ based on interference model, due to σ_z^2 in equation (2.7b). This method is used in Chapter 3 of this thesis, and in Publications I and II.

2.2 Interference characterization

The main quantity of interest in this section is the aggregate interference. The amount of the aggregate interference can be broadly expressed as the sum of the received power levels from individual nodes

$$I \quad = \quad \sum_{k \in \Phi} v_k \cdot P_k \cdot L_k \tag{2.9}$$

where v_k is a binary variable describing whether the k-th node is active or not, P_k is the transmit power level, L_k is propagation pathloss including fading coefficient from k-th node, and $\Phi \subset \mathcal{R}^n$ denotes the set of the potential interferers on the same frequency band. The transmit power level P_k $\forall k$ and the spatial distribution of the interferers determine the interference to the first-order, while the fading effect is smaller but certainly non-negligible [37]. The spatial distribution depends on the network topology and the medium access control layer protocol. Thus, the aggregate interference can be controlled by a power allocation scheme which sets appropriate constant power level to the active transmitters, and by the medium access control scheme which controls the access of the

underlying network nodes to the shared spectrum.

There are two different network deployments which are deterministic, i.e., fixed locations of nodes such as a cellular downlink system, and random, i.e., random locations of nodes such as WLAN users, D2D users, vehicles, and uplink cellular users. In random deployment, there are broadly two channel access schemes determining the active users who are located in spatially independent, i.e., either contention-free multiple access or random access without contention control (Aloha-type MAC), and who are located in spatially dependent, i.e., random access with contention control (CSMA-type MAC). In the following subsections, the aggregate interference is characterized by methods based on stochastic models where the properties of the fading, or the positions of nodes, are considered as random processes with specified probability distribution.

2.2.1 Deterministic interferers

While regular deployment does not provide analytical tractability, this model has been helpful in the numerical studies of macro-cellular networks. Such deterministic placement of nodes may be applicable where the locations of nodes are known or constrained to a particular structure. In this case, the randomness at the aggregate interference is only caused by a fading effect. Thus, modeling the aggregate interference in the deterministic network can be interpreted as modeling the distribution of the sum of RVs used to model the fading from each transmitter.

Slow fading is usually modeled by a Lognormal RV in a static network, i.e., a TV broadcasting system or secondary cellular system downlink in TVWS, where the effects of small-scale fading can be averaged out and slow fading dominates such slow fluctuations in the generated interference levels. Due to this fact, it is of fundamental importance to find the distribution for a sum of lognormally distributed RVs. A closed-form expression of the LT of the Lognormal distribution does not exist. However, it has been recognized that the Lognormal sum can be well approximated by a new Lognormal RV (Method #1 in Section 2.1.1). Thus, the problem is now equivalent to estimating the Lognormal moments given the corresponding statistics of the Lognormal RVs (See Chapter 3).

2.2.2 Independent and random interferers

In the Aloha-based access method, nodes transmit their packets without any coordination between them, while the cross-tier interference can be controlled. Due to the spatially uncorrelated locations of the nodes, the spatial distribution of randomly located nodes with Aloha-type MAC can be captured by the PPP model where the number of nodes at any time instant is drawn from a Poisson RV with a mean equal to the PPP density λ_p and the coexisting nodes are uniformly deployed within the service area of interest.

The exact LT for the aggregate interference in the PPP field can be obtained by using the PGFL of the PPP [37]. The LT for the aggregate interference generated to a receiver located at an arbitrary location in $\mathcal{R}^n$, associated with an infinite PPP and no exclusion regions around the receiver, corresponds to the LT of an alpha-stable distribution [38]. However, it is non-trivial to deal with the skewed-stable distributions, since the inverse transform of the LT can be expressed in a closed-form only for a pathloss exponent equal to 4 in [39] for no fading, and in [40] for Rayleigh fading. The expression for the LT of the aggregate interference generated in finite and spatially non-symmetric deployment due to the existence of exclusion regions around the receivers in an inter-system spectrum sharing scenario, e.g. secondary spectrum access in TVWS, can have a complex form, and thus generally does not admit closed-form solutions for the PDF.

One approach to solve the problem is to approximate the distribution of the aggregate interference by a suitable distribution (See Method #1 in subsection 2.1.1). The distribution of aggregate interference is approximated by the Gaussian distribution in [41, 42] under the bounded (non-singular) pathloss model or protection region around the receiver. The distribution of aggregate interference has been approximated by Lognormal distribution [43], shifted Lognormal distribution [43,44], truncated stable distribution [45], the Gamma and inverse Gamma distributions [37], and the inverse Gaussian distribution [46]. The other alternative has to be numerically inverted to compute the exact PDF of the aggregate interference. However, this approach is not pursued in this thesis as it is computationally intensive and offers little insight into the relation between the aggregate interference and its effect on performance metrics.

2.2.3 Dependent and random interferers

In the CSMA-based access method, nodes simultaneously cooperate and compete for spectrum access, while the cross-tier and intra-tier interferences are controlled. Since the locations of the simultaneously active nodes are correlated, the spatial distribution randomly located nodes with CSMA-type MAC can be captured by the MPP [47], instead of the PPP. The MPP is a repulsive point process where no two points of the process can coexist within a distance less than the Hardcore Distance (HCD) δ. That is, MPP correlates the locations of the points by conditioning on a minimum distance separating them. There are different types of MPPs distinguished based on the rule that governs the selection of effective points, i.e., the points that survive the thinning of the PPP. The probability that a point of the PPP is retained and becomes effective is highest for MPP type III and lowest for MPP type I [48]. No exact results exist so far for the retaining probability in MPP type III [49], while the retaining probabilities in MPP types I and II are available in closed-form.

While the exact LT of the aggregate interference is available for the PPP, it is unavailable for the MPP due to the nonexistence of the PGFL. This intractability has been resolved by the approximation that the nodes further away than δ can still be modeled as a PPP [29], which would make the analysis of CSMA networks fairly tractable, but only valid for evaluating cross-tier interference generated from spatially uncorrelated tiers. A common practice for computing the cross-tier aggregate interference at an arbitrary point on the plane is to approximate the MPP by using a homogeneous equi-dense PPP [50]. For parent density λ_p, the density of the MPP type II process is as follows [20]

$$\lambda_m = \frac{1 - e^{-\lambda_p \pi \delta^2}}{\pi \delta^2}. \tag{2.10}$$

The moments of the aggregate interference from a MPP type II process can be computed after replacing λ_p with λ_m. However, such an equi-dense PPP approximation method is not valid for finite deployment, due to the existence of borders [50]. In particular, designing the CS range based on the PPP approximation will violate the protection of the primary receivers. One way to overcome this issue is to bound the mean interference by using a multi-tier PPP (see Chapter 3).

According to Slivnyak's theorem, the Palm distribution of a PPP coincides with the distribution of the original PPP [20], which is not valid

for a hardcore point process. As a result, the aggregate interference at a particular node of the process should be handled differently from the one at an arbitrary point on the plane. The self-interference in hardcore wireless networks is computed by using Palm distribution and moment measures [37]. For instance, the mean interference at a particular node is studied based on the fact that the point pattern for a MPP is the result of a mixture of the first-order density and second-order density functions.

Given a transmitter, there are two types of transmitters generating interference at the reference transmitter and its associated receiver. They are separated based on their distances from the reference transmitter. Since two transmitters separated by 2δ are uncorrelated, the MPP type II behaves like a PPP for a distance separation higher than 2δ. On the other hand, two transmitters separated by less than 2δ are correlated. The correlation property can be captured by the PCF [20], the normalized version of the second-order density function, which has a complex form. The bounds of the PCF have been derived in [29] and more accurate bounds are presented in Publication III.

The amounts of the aggregate interference at a transmitter and a receiver are used to perform the CCA and to evaluate a target link performance, respectively. An upper bound on the interference at the receiver underestimates the SINR and can be used to obtain a lower bound on the performance. A lower bound on the interference at the transmitter underestimates the CS threshold. That reduces the density of active transmitters and means less cross-tier interference to other systems in a different tier, i.e., protecting the primary system in secondary operation (see Chapter 3). On the other hand, if the inactive transmitters after the CCA are handed over to a different operating mode, the upper bound on the interference at the transmitter is in favor of the QoS in the mode, i.e., in cellular communication mode selected by threshold-based mode selection for D2D communication (see Chapter 4).

3. Database-assisted secondary system in TV white space

In this chapter, we consider spectrum sharing between a TV system and a secondary system in LSA mode. We focus on low-complex algorithms to enable a real-time operation in geolocation database-assisted secondary spectrum access where cross-tier interference at a TV system is limited and strong self-interference at the licensed secondary system is avoided.

3.1 Introduction

White spaces in the Ultra High Frequency (UHF) TV bands have been of particular interest [51–53] due to their low utilization and excellent propagation characteristics as compared to the higher frequency bands. Secondary systems allowed to use the TV spectrum can enhance the spectrum efficiency and alleviate the spectrum scarcity. One of the main requirements for secondary operation in the TVWS is to maintain the QoS in the TV system. The transmissions in TVWS are conditioned by regulators on the ability of the secondary system to avoid harmful interference to incumbents. To this end, the general consensus among the Federal Communications Commission (FCC) [51], Electronic Communications Committee (ECC) [52], and Federal Office of Communications (OFCOM) [53] is on the adoption of database-assisted spectrum sharing architecture [54]. The geolocation database, as a centralized controller, provides the list of available TV channels, and controls some operational parameters, enabling management of the cross-tier interference between the incumbent TV system and the secondary system, based on the protection criteria of the primary system.

While the secondary systems access the primary spectrum mainly with the protection of incumbent services, they should also experience sufficient performance as in LSA mode [8]. Otherwise, the benefits of exploit-

ing the primary spectrum are limited and secondary spectrum sharing is not a viable option. The gains for the spectrum sharing are constrained by the amount of the interference among the secondary nodes. Therefore, the secondary self-interference as well as the cross-tier interference should be taken into account, and both can be controlled by the operational parameters determined by the associated rules. To this aim, the secondary systems would use the TV spectrum under individual authorizations for a specific local area in line with the LSA concept where the operation in LSA mode is possible without interfering with the TV system as long as it follows the rules or algorithms set by the geolocation database [9–12], i.e., the LSA Repository/Controller in the LSA model.

The LSA can make use of recent progress in secondary spectrum access methods [55]. Different rules for secondary transmit power allocation have been selected in the US by the FCC [16, 51] and in Europe by the ECC [15, 52]. The FCC specifies a fixed transmission power level allocation with a protection distance around the TV coverage area. On the other hand, in the ECC, a location-based transmission power allocation rule is used: the further the secondary node is located from the TV cell border the higher transmission power it can utilize. Because of that, a high signaling overhead between secondary transmitters and the database is required for the location based algorithm. Unfortunately, the current rules do not provide any secondary performance guarantees, since the self-interference is not taken into account. Furthermore, they are not able to protect the primary system service in all cases [56].

The potential of WiFi-like technology in TVWS has triggered the development of new wireless standards like the IEEE 802.11af [57], and the ECMA-392 [58] in TVWS. The ECMA-392 provides a CSMA-type MAC in TVWS, which permits multiple devices to contend for medium access. A node does a CCA check before using the channel and during CCA observation time the energy in the channel is measured and compared to a CS threshold. An adaptive CS threshold can be used for the protection of a TV system and more effective spectrum sharing in TVWS [8], since it determines the number of active secondary nodes and the minimum distance among nearby active nodes, affecting the cross-tier interference and self-interference, respectively. In general, the threshold value is common to all users. Thus, it is challenging work to obtain the common parameter.

In this chapter, we present the main methods and results of Publications I and II. The aim of the methods is to control secondary generated

interference toward the primary system by properly allocating the transmit power for a cellular downlink system and setting the CS threshold for a WLAN system employing a CSMA-type MAC. The results can be summarized as a power allocation algorithm for a cellular downlink system in TVWS, incorporating secondary self-interference constraints for the coverage of the licensee in LSA mode, and a low complexity mechanism to set a CS threshold for a WLAN system with a CSMA-type MAC, considering the existence of borders and protection regions between the two systems. The details of the analysis and more results can be found in Publications I and II.

3.2 System model

We consider a TV transmitter located in the center of a circular TV service area and a secondary system deployed outside of the TV protection area. The secondary system operates on a co-channel to the TV transmitter. A cellular system and a WLAN system are considered as candidates for secondary spectrum access. The main performance metric for the scenario of the secondary spectrum access to the TV system is to maintain satisfactory quality for the primary service. For satisfactory TV reception a target SINR γ_t at a TV receiver must be maintained with specific outage probability O_t, i.e., secondary transmissions are allowed if the condition in (2.2) is satisfied in the presence of secondary transmissions [59]. Assuming that both the useful TV signal and the aggregate secondary interference follow the Lognormal distribution, the condition can be converted to a chance type of constraint in equation (2.8) by using Method #3 in Section 2.1.3.

3.3 Interference model

In this section, we discuss interference models for secondary systems. In order to model the secondary interference by the FW method, the first two moments of the aggregate interference are computed. A straightforward approach to an aggregate interference model is to sum up all the interfering powers at a TV test point. For equal transmit power levels, $P_k = P$, and i.i.d. fading samples, the first two moments of the interference can be

expressed as

$$E[I^{SU}] = P \cdot E[x] \cdot \sum_{k \in \Phi^{SU}} l_k \tag{3.1i}$$

$$E[{I^{SU}}^2] = P^2 \cdot \left(E[x^2] - E[x]^2\right) \cdot \sum_{k \in \Phi^{SU}} l_k^2 + E[I^{SU}]^2 \tag{3.1ii}$$

where Φ^{SU} is the set of active secondary transmitters, i.e., cellular downlink BSs or WLAN users, l_k is the mean pathloss from transmitter k to the TV test point, and in each path the mean fading loss is the same, $E[x] = E[x_k], \forall k$.

Such direct summation requires information about the secondary transmit power and its location for calculation of the attenuation to the primary test point. When there are a large number of secondary transmitters in TVWS, this approach causes high computational overhead, and communication signaling overhead for updating the changed locations in the database if the locations of the secondary transmitters, i.e., WLAN users, are changed frequently. One way to reduce such overhead is to approximate the summation in the above equation by integrating the secondary transmission area, S: $\sum_{k \in \Phi^{SU}} l_k = \frac{1}{S_f} \int_S l_s ds$ where S_f is the footprint of one transmitter and has only one active transmitter.

3.3.1 Interference from cellular downlink system

For the downlink of a cellular system, the footprint contains the cell area. The ratio of transmit power divided by the footprint is the spatial power density $P_d = \frac{P}{S_f}$. For a constant power density over area S, the equations (3.1) can be read as follows [60]

$$E[I^{SU}] = P_d \cdot E[x] \cdot \int_S l_s ds \tag{3.2i}$$

$$E[{I^{SU}}^2] = P_d^2 \cdot \left(E[x^2] - E[x]^2\right) \cdot S_f \cdot \int_S l_s^2 ds + E[I^{SU}]^2 \tag{3.2ii}$$

where l_s is the distance-based propagation pathloss from the integration element of area S to the primary test point.

3.3.2 Interference from WLAN system

For a WLAN system with an Aloha-type MAC, secondary transmitters can be located anywhere in the deployment S. When k number of transmitters are uniformly distributed over the area S, modeled by a Binomial Point

Process (BPP), the spatial power density becomes $P_d = \frac{P}{S/k} = \frac{k \cdot P}{S}$. The first two moments for a BPP can become [60]

$$E[I_b] = \frac{k}{S} \cdot P \cdot E[x] \cdot \int_S l_s ds \tag{3.3i}$$

$$E[I_b^2] = \frac{k}{S} \cdot P^2 \cdot E[x^2] \cdot \int_S l_s^2 ds + \frac{k-1}{k} \cdot E[I_b]^2 \tag{3.3ii}$$

When the average number of transmitters follows Poisson distribution with mean $\lambda_p S$ where $\lambda_p = k/S$, the spatial power density becomes $P_d = \lambda_p \cdot P$. The first two moments for a PPP are [60]

$$E[I_p] = \lambda_p \cdot P \cdot E[x] \cdot \int_S l_s ds \tag{3.4i}$$

$$E[I_p^2] = \lambda_p \cdot P^2 \cdot E[x^2] \cdot \int_S l_s^2 ds + E[I_p]^2 \tag{3.4ii}$$

Note that, conditioned on there being exactly k number transmitters present, the PPP is equivalent to a BPP [20]. One can see that the moments of the BPP in equation (3.3) are equivalent to the moments of the PPP in equation (3.4), if the number of transmitters k and the area size S increase such that the ratio k/S remains constant, equal to λ_p.

For a WLAN system with a CSMA-type MAC, the secondary transmitters are also randomly located but there is spatial dependence among the transmitters due to the mutual exclusion scheduling where no other transmitter in the exclusion regions can transmit concurrently. As discussed in Chapter 2, the set of active transmitters with a CSMA-type MAC can be captured by a hardcore process, MPP type II.

For the cross-tier aggregate interference at an arbitrary point, the MPP can be approximated by an equi-dense PPP [29]. By using the PPP approximation, the moments of the aggregate interference from the MPP process can be obtained from replacing λ_p in equations (3.4) with λ_m in equation (2.10). However, in a primary - secondary system setup, there are exclusion areas around every primary receiver and the active node density close to the borders is higher than λ_m due to less contention. As a result, setting the common HCD based on a homogeneous PPP with density λ_m will violate the protection criteria at the TV receiver. The PPP approximation worsens for increasing parent density λ_p and increasing HCD δ.

The secondary deployment area can be divided into two disjoint regions S_1 and S_2, $S = S_1 \cup S_2$ (see Figure 3.1(a)). The interference generated by each region to the TV receiver is approximated by a PPP. The densities of

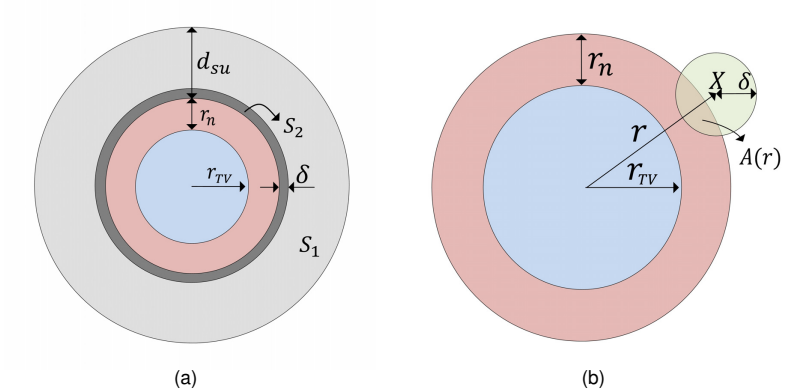

Figure 3.1. Illustration of (a) two disjoint regions in the secondary deployment area and (b) border effect.

the PPPs in the two regions are λ_m for $r \geq (r_{TV}+r_n+\delta)$ and λ_2 for $r_{TV}+r_n \leq r < r_{TV}+r_n+\delta$, respectively. The moments of the aggregate interference can be computed a sum of the moments over the disjoint areas

$$E[I^{SU}] \approx \lambda_m \cdot P \cdot E[x] \cdot \int\limits_{S_1(\delta)} l_s ds + \lambda_2 \cdot P \cdot E[x] \cdot \int\limits_{S_2(\delta)} l_s ds \tag{3.5i}$$

$$E[{I^{SU}}^2] \approx \lambda_m \cdot P^2 \cdot E[x^2] \cdot \int\limits_{S_1(\delta)} l_s^2 ds + \lambda_2 \cdot P^2 \cdot E[x^2] \cdot \int\limits_{S_2(\delta)} l_s^2 ds + E[I^{SU}]^2 \tag{3.5ii}$$

where the areas S_1, S_2 are functions of the HCD δ. Next, we obtain the density λ_2 by looking at the simple geometrical dependency in Figure 3.1(b), the density is upper bounded by

$$\lambda_2 = \frac{1 - e^{-\lambda_p(\pi\delta^2 - A(r_{TV}+r_n))}}{\pi\delta^2 - A(r_{TV}+r_n)} \tag{3.6}$$

where $A(r)$ is the intersection area of two circles whose centers are at distance r. Since $r_{TV}+r_n \gg \delta$, $A(r_{TV}+r_n) \approx \pi\delta^2/2$. The density λ_2 becomes

$$\lambda_2 \approx \frac{1 - e^{-0.5\lambda_p\pi\delta^2}}{0.5\pi\delta^2} \tag{3.7}$$

3.4 Interference control

With interference model tailored to the primary-secondary system setup at hand, we can look for methods to control aggregate interference. To achieve this, in this section, we focus on two interference control algorithms, through allocating transmit power to a cellular downlink system

and setting the CS threshold to a WLAN system with contention control.

In order to protect the primary system, equation (2.8) can be treated as the necessary condition for interference control. It is a complex function due to non-linearly involved secondary system parameters. For a simplified interference margin, we utilize the fact that the aggregate interference level is an order of magnitude less than the useful TV signal level, and the assumption that all the interfering signals have the same fading variance. The approximation tightness for the lower bound of the interference margin can be provided, $I_{\triangle_l} \leq I_{\triangle}$, which was first established in [34] and verified in [61]. By using the lower bound of the interference margin $I_{\triangle_l}$, the constraint (2.2) can be turned into a simplified constraint

$$E[I^{SU}] \leq e^{\frac{\sigma_W}{\xi}Q^{-1}(1-O_t)-\ln(\gamma_t)+\frac{\mu_W}{\xi}} - N \doteq I_{\triangle_l} \tag{3.8}$$

where $I_{\triangle_l}$ is a function of only the primary system parameters, $\mu_W, \sigma_W, \gamma_t$ and N. To satisfy the interference constraint (3.8), the geolocation database can allocate some operational parameters, i.e., transmit power level or CS threshold value, to the secondary system.

3.4.1 Transmit power to cellular downlink system

Any viable power allocation algorithm must meet the secondary spectrum access constraint (3.8) on one hand and optimize the performance of the secondary system on the other. Given the allocated interference margin for multiple secondary transmitters, different utilities can be optimized. Weighted sum rate maximization can be considered as a natural utility, subject to a primary constraint [62].

In Publication I, the sum cell border data rate of the secondary network is selected to be the optimization objective, subject to a primary constraint as well as a secondary cellular coverage constraint. We consider K_c cellular cells, T_1 test points along the TV coverage, and T_2 test points over the secondary deployment. The power allocation scheme is formulated as the optimization problems

$$\underset{\mathbf{P}}{\text{Maximize}} : w\sum_k \sum_p \log_2(1+\gamma_{k,p}(\mathbf{P})) \tag{3.9i}$$

$$\text{Subject to} : \quad \mathbf{L}_1 \cdot \mathbf{P} \leq \mathbf{I}_{\triangle_l}^{(PU)} \tag{3.9ii}$$

$$\mathbf{L}_2 \cdot \mathbf{P} \leq \mathbf{I}_{\triangle_l}^{(SU)} \tag{3.9iii}$$

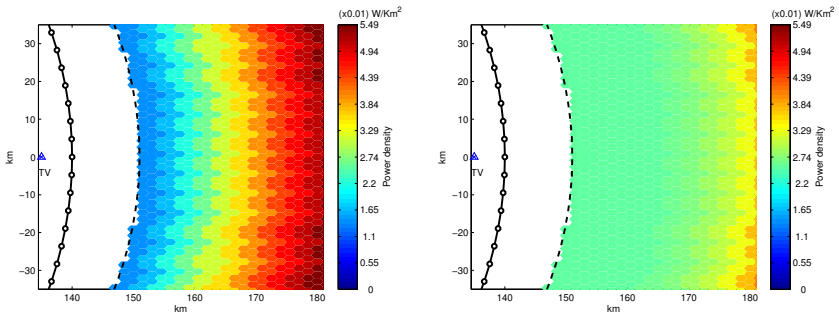

Figure 3.2. (a) TV protection constraints and (b) TV and secondary protection constraints. Spatial power density emitted from the secondary deployment area. Secondary transmitters are placed on a cellular lattice with reuse 3. TV SINR target is 17.1 dB and secondary SINR target is -3.5 dB. Target outage probability for TV and secondary system is 10 %. The HATA model for secondary propagation pathloss has been used.

where w are non-negative weight, $\gamma_{k,p}(\mathbf{P})$ is the SINR at the p-th test point of the k-th secondary cell, $\mathbf{L}_1$ and $\mathbf{L}_2$ are the matrix of mean link gains including slow fading from the secondary interfering transmitters to the TV test points and the secondary test points, respectively, with $T_1 \times K_c$ and $T_2 \times K_c$ elements. $\mathbf{I}_{\triangle_l}^{(PU)}$ and $\mathbf{I}_{\triangle_l}^{(SU)}$ are column vectors of interference margins available at the TV test points and the secondary test points calculated by following steps similar to the ones used for equation (3.8), with T_1 and T_2 elements.

In Figure 3.2, difference in power allocation with and without secondary constraints for a cellular secondary system in TVWS is illustrated. With only TV constraints in equation (3.9ii), the secondary downlink sum rate is maximized in a similar way as with a Proportional Fair (PF) power allocation rule [63] where the secondary transmitters equally consume the available interference margin. The less the link gain to the TV test points, the higher the allocated transmission power (see Figure 3.2(a)). Even if the PF power allocation scheme is similar to the rule in ECC [15], it is able to protect the TV service in all cases. However, such fairness in secondary operation introduces real-time implementation issues in a number of secondary transmitters. The geolocation database should operate with low complexity algorithms in order to handle frequent spectrum access requests in real time. To resolve the issue, a sub-optimal method with low complexity is proposed in [63].

With TV constraint and cellular coverage constraints equations (3.9ii) and (3.9iii), the transmission power levels allocated to secondary cells close and far from the TV cell border are about the same. Secondary cells

located close to the primary system suffer more from the generated primary interference and they have to utilize higher transmit power levels to meet their own SINR constraints. As a result, less of a TV interference margin is allocated to secondary cells located further away, and the power allocation looks almost uniform (see Figure 3.2(b)). Such a uniform power allocation rule gives an opportunity to quickly obtain an insight on the impact of various parameters on the cellular data rate and the TV protection criteria, thanks to its low complexity. The observation can deduce that since the FCC rule suggests the use of constant power [16], it captures the general trend better than the ECC rule. However, it should be based on the interference margin available at the primary and secondary test points.

3.4.2 CS threshold to WLAN system

An efficient MAC protocol of the secondary system in TVWS is essential for achieving successful secondary access, since it has a large impact on the secondary generated aggregate interference in the primary system. For instance, increasing the CS threshold decreases the CS range and, subsequently, increases the density of active users while at the same time increasing secondary generated self-interference. In order to achieve a balance between spatial reuse and data rate, a method to tune the CS threshold is proposed in [64], but it is only valid within a single system. The impact of CS range on the interference generated in the primary system is identified in [50]. However, there is no proposed algorithm neither for setting the CS range so that the primary system is safely protected nor for mapping the CS range to a CS threshold.

Due to the similarity to the CSMA-type MAC, a MPP type II process is commonly employed to model the locations of active transmitters in wireless networks with contention control (See Chapter 2). Note that while a retaining probability in a MPP is determined by a HCD, a retaining probability in a wireless network depends on a CS threshold. In Publication II, we first show i) how to set the HCD in MPP networks without violating the condition $E[I^{SU}] \leq I_{\triangle_l}$ in equation (3.8) and then ii) how to map the identified HCD to the CS threshold which is a common parameter to control the activity of the secondary network.

Setting HCD

The active densities λ_m and λ_2 of two PPPs modeling secondary transmitters over the areas S_1 and S_2 in Figure 3.1(a) are identified in order to calculate the cross-tier interference in equation (3.5) and to satisfy the interference margin $I_{\triangle_l}$ in (3.8). The densities can be obtained by a tight upper bound for the HCD δ protecting the TV service. To resolve no closed-form solution in terms of the HCD in equation (3.5), two steps are proposed for a tight upper bound for the HCD. We first find a tight lower bound δ_l assuming PPP with density λ_m inside full area S and forcing the inequality $E[I^{SU}] \leq I_{\triangle l}$ to be tight, which can be expressed in terms of the principal branch $\mathcal{W}_0(t)$ of the Lambert function [65] $\mathcal{W}(t)$ representing exactly one real solution of the equation $t = \mathcal{W}(t)e^{\mathcal{W}(t)}$ for all real $t \geq 0$

$$\delta_l = \begin{cases} 0 & \text{if} \quad \lambda_p \leq I'_{\triangle_l} \\ \sqrt{\frac{1}{\pi I'_{\triangle_l}} + \frac{1}{\pi\lambda_p}\mathcal{W}_0\left(-\frac{\lambda_p}{I'_{\triangle_l}} \cdot e^{-\frac{\lambda_p}{I'_{\triangle_l}}}\right)} & \text{if} \quad \lambda_p > I'_{\triangle_l} \end{cases} \tag{3.10}$$

where $I'_{\triangle_l} = I_{\triangle_l}/(P \cdot e^{\sigma^2/2\xi^2} \cdot \int_S l_s ds)$, and then ii) a tight upper bound is numerically identified by increasing the HCD with discretization step $\triangle\delta$ until the constraint $E[I^{SU}] \leq I_{\triangle l}$ is satisfied. The proposed upper bound is tight and few iterations would be sufficient to compute it. The implementation complexity can be reduced by storing the integration results and evaluating offline the integral $\int_S g_s ds$.

Setting CS threshold given HCD

In order to map the HCD to a CS threshold we need to compute the mean self-interference at a node in hardcore wireless networks, e.g., MPP types II and III. Due to the dependent property of MPP, the calculation of mean interference at a node in a MPP type II involves the integral of the PCF [20], which does not accept a closed-form. In order to bypass the complex numerical integration, a lower bound on the mean interference at a transmitter is used, which underestimates the CS threshold and protects the primary system. In MPP type III, the mean number of active nodes cannot be described in closed-form even, unless the parent density λ_p goes to infinity [66] due to no closed-form expressions for first and second-order moment properties [48]. For finite secondary user densities we can only look for bounds to the mean number of survived nodes in a MPP type III. Due to the analytical tractability of MPP type II, we need to upper bound the number of points generated from a MPP type III by using a MPP type

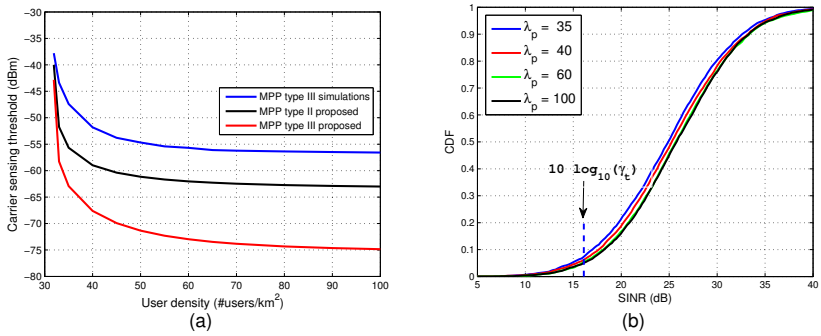

Figure 3.3. (a) CS threshold set by the proposed methods for MPP types II and III [48], and the simulation by a modified version of the SSI model [66] (b) SINR distributions at the primary test point, generated using the CS threshold for the MPP type II. Note that the outage probability at the SINR target would be equal to the outage probability target 10% for the simulated thresholds.

II. A tight bound is difficult to derive because MPP type III is complex to analyze. One simple but loose upper bound suggests doubling the HCD of the MPP type II process [48].

In primary-secondary setup, the mean interference is different at different locations of the secondary deployment area due to the existence of borders. In order to use a common CS threshold for interference control, we calculate the mean interference for a reference transmitter located at the primary protection area border. Since a node at the border is exposed to less interference, the CS threshold is underestimated and the TV system is further secured.

In Figure 3.3(a), the proposed methods result in a smaller CS threshold than the simulations mainly due to the following two reasons: (i) the calculated HCD for the MPP type III has been doubled and (ii) the threshold has been set based on the interference level at the protection area border. The results of Figure 3.3(b) illustrate the reduction in outage probability due to the conservative approximations adopted by our proposal. For high user densities where the active node density is about half the maximum permitted, the outage probability is about 5%.

The presented CS threshold is seen as a common parameter to control the activity of the secondary network. The proposed method has low complexity and makes it possible to compute the CS threshold in real-time. As a result, the method can be utilized in geolocation database-assisted secondary spectrum access even in cases there are frequent changes in secondary user density.

3.5 Discussion

In this chapter, we discussed secondary spectrum access in the TV spectrum using the geolocation database. For secondary spectrum usage, the TV service should be primarily protected. To reach this target, the available interference margin at the TV test points is first calculated [34], which is the amount of permitted secondary interference, a similar concept as interference temperature [67]. The interference margin was treated as an available resource. Based on its share of the margin, a database can allocate some operational parameters to a secondary system, taking the benefits of secondary spectrum access into account, as in LSA mode.

The current power allocation rules proposed by the standardization bodies in the US and EU for secondary spectrum access in TVWS do neither protect the TV service in all cases [55, 56, 68], nor guarantee sufficient secondary performance. In Publication I, for cellular systems in TVWS, we proposed a low-complex power allocation algorithm incorporating secondary self-interference constraints. We illustrated that the optimal power density allocation tends to be uniform under secondary cellular coverage constraints. The uniform approximation reduces the amount of computations, making it possible to assess the amount of available TVWS capacity in Finland. Our results agree with the findings presented in [69].

The CS threshold adaptation in CSMA-based wireless networks plays an important role in the interference management and performance enhancement [70], but not directly applicable in a primary-secondary system setup. The CS threshold in secondary wireless networks can be viewed as a parameter that can be tuned to set the maximum number of licensed secondary users and some pairwise inter-user distance separation, limiting the cross-tier interference at primary system and avoiding strong self-interference in secondary system in LSA mode. However, it is not easy to find a proper common CS threshold due to the existence of borders where the density close to the borders is higher due to less contention, and the amount of the self-interference is different at different locations in secondary deployment. In Publication II, we proposed a low complexity method for setting the CS range by using MPP, and mapping it to a CS threshold given the maximum density of transmitters in two disjoint secondary regions.

Note that MPP is practically used to maintain a density of users and a

minimum distance separation between users in an attempt to capture real deployments of a WLAN system [47, Table 1]. Some effort has been made to model the interference as function of different types of MPP models and modified version of the Simple Sequential Inhibition (SSI) model [66], and to validate them by the network simulator [71]. Even if the MPP seems realistic, it suffers flaws such as a spatial anomaly in high density, resulting in an underestimation in the number of transmitters and in the resulting interference level. The modified version of the SSI model seems the most suited to offer a realistic model of a wireless network with a CSMA-type MAC. However, little is known about the SSI processes for analytical purposes, therefore increased accuracy comes at the expense of less analytical tractability.

Note that our proposed method for MPP type III sets the CS threshold conservatively, due to several approximations for setting conservatively both the HCD and the CS threshold. Given our parameter settings, doubling the HCD reduces the CS threshold by 12 dB in comparison with the threshold calculated based on the MPP type II. In order to enable a higher density of secondary transmitters, we need to identify a tighter upper bound for the number of points survived in a MPP type III. The proposed method of MAC layer can be further improved by incorporating physical parameters such as transmit power [72] or transmission rate [73].

Note that the secondary performance needs to be estimated to gain a glimpse of the viability of secondary spectrum access, while the primary system is protected. There are some studies related to the performance of secondary networks with the CSMA-type contention control [74], [75]. However, the performance evaluation ignores the impact of aggregate secondary interference on the primary system which is not protected by any CS threshold. In [76], the data rate of the secondary system is investigated with a CS threshold protecting the primary system. The gap between the method and simulation exists due to the underestimation problem of MPP type II. Nevertheless, the method still allows estimation of the secondary performance and assessment of the relation between the secondary performance and the primary protection constraints. Interestingly, small relaxation in the protection constraints can result in significant benefits on the secondary system side. However, after a certain point, the secondary performance becomes limited due to self-interference.

4. Device-to-Device Communications

In this chapter, we consider co-primary spectrum sharing for direct communication between two users subscribed to different operators. We aim to identify how much spectrum each operator should commit for direct communication, and to design a mechanism with low complexity and signaling overhead for managing cross-tier as well as intra-tier interference. The tier levels are differentiated from different link types such as cellular links and direct links within an operator, and the direct link between two nodes subscribed to different operators.

4.1 Introduction

D2D communication has been developed as a promising technology to meet the demands for spectrum utilization and high data rate services by enabling a direct link between two end users in close proximity [77, 78]. The D2D communication paradigm has been largely exploited in non-cellular technologies such as Bluetooth or WiFi direct in the ISM band. However, due to the unpredictability of the interference in unlicensed bands, it has not yet been fully incorporated into existing cellular networks.

Integrating D2D communication into LTE-A has been recently approved by the 3GPP community [79]. Such integration requires that the interference be managed carefully [80], because the introduction of D2D communications should not affect the performance of existing cellular communication, and also its applicability should not be limited by the transmissions of cellular and/or other D2D pairs. Essentially, the main technical challenges for the interference issue arise from the following aspects: the random spatial location of both cellular and D2D users, and the operation complexity in terms of signaling overhead. For instance, the BS has to

know the Channel State Information (CSI) of all involved links for efficient interference and resource management. However, its exchange is very demanding in terms of signaling due to the random spatial location of both cellular and D2D users, which will dominate the available radio resource in a random dense network.

Co-primary spectrum sharing can be used for inter-operator D2D communication, when two end users of a D2D pair who have subscriptions with different operators want to communicate directly [81, Section 4.1], and the communication should take place over the licensed spectrum of the operators [82, 83]. This scenario is extremely complicated in terms of controlling interference due to the need for coordination between involved operators. For instance, information exchange between the operators might be needed to resolve the interference generated from inter-operator D2D links to cellular nodes or intra-operator D2D users. Also, it is non-trivial to identify the amount of spectrum each operator contributes to a shared band for inter-operator D2D communication. Participating operators can obtain the benefits, i.e., fair and efficient spectrum allocation, by exchanging some information. However, operators are essentially competitors, and thus may not want to reveal operator-specific information to others.

In this chapter, we present the main methods and results of Publications IV, V, and VI. The aim of the methods is for interference control and spectrum allocation for D2D communication. The considered approach enables the coordinated common usage of dedicated spectral resources by users from different operators, and co-primary spectrum sharing gain is achieved. The results can be summarized as i) mechanism with low communication signaling overhead between D2D users and BSs in dense deployments for interference control and spectrum allocation, and ii) a co-primary spectrum sharing solution with limited information available to each operator. The scheme for allocating spectrum for inter-operator D2D communication is presented in the TeC14 of METIS deliverable D5.4 [9]. The details of the analysis and more results can be found in Publications IV, V, and VI.

4.2 D2D radio resource allocation and communication modes

The nodes such as BS, cellular user and D2D user are affected by interference, depending on resource allocation mode and communication mode for

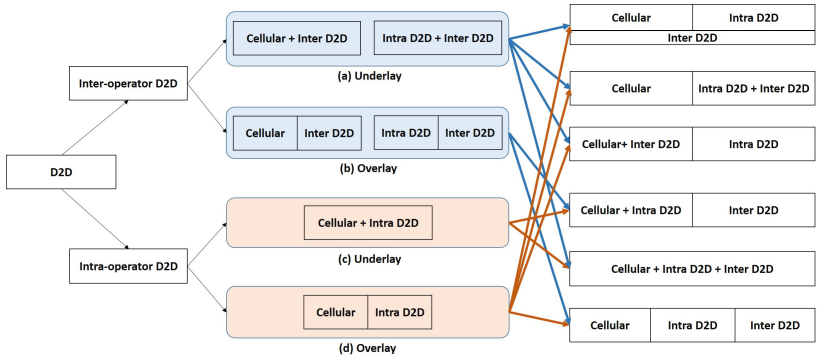

Figure 4.1. Radio resource allocation mode for D2D communication.

D2D communication. Communication mode identifies whether D2D users communicate via the BS (cellular mode) or directly with each other (D2D mode), based on the decision of the proper mode selection algorithm. Furthermore, resource allocation mode distinguishes if D2D communication uses the same radio resources as the conventional cellular communication or not. D2D mode and cellular mode can operate over the same resources (D2D underlay), or dedicated spectrum can be allocated to the D2D mode (D2D overlay).

4.2.1 Radio resource allocation mode

The D2D underlay mode increases the spectral efficiency at the expense of cross-tier interference (see Figure 4.1). (a) The cross-tier interference between different operators, i.e., between cellular and inter-operator D2D links, or between intra-operator D2D and inter-operator D2D links, can be resolved by information exchange between the operators. Due to the fact that operators may not be willing to reveal proprietary information, D2D overlay mode for inter-operator D2D links would be easier to implement. (c) The cross-tier interference within a single operator, i.e., between cellular and intra-operator D2D links, can be managed by the BS, through properly coordinating D2D and cellular transmissions. To do so, the BS has to know the CSI of all involved links but the BS's participation to make scheduling decision causes large signaling overhead especially in dense deployments.

The D2D overlay mode, on the other hand, eliminates (b) cross-tier interference between different operators, and (d) cross-tier interference within the same operator. These approaches enjoy more spectral efficiency than the case where D2D communication does not operate. However, the cel-

lular spectrum might be used inefficiently due to the fixed spectrum allocated to the D2D overlay mode. One way to improve spectrum utilization is to use proper mode selection algorithms which would determine the actual density of D2D transmissions, coupled with spectrum allocation for D2D communication in the system design.

While most of the available D2D related works have focused on intra-operator D2D communication in D2D underlay mode and/or D2D overlay mode [84–92], the available studies for inter-operator D2D can be found in [93, 94] where the patents designed D2D discovery protocols [93] and D2D broadcast communications [94]. However, they are not seen to address how much spectrum should be allocated on a co-primary sharing basis for inter-operator D2D communication. Inter-operator spectrum sharing has been addressed in [83] where different operators allocate a different amount of resource for active RAN sharing, since they may have different demand. However, they do not propose any algorithm determining the amount of spectrum allocated to each operator, and also they do not address the requirements on inter-operator spectrum sharing for D2D communication.

The overlay inter-operator spectrum sharing can be implemented with a cooperative or non-cooperative game approach to determine the amount of spectrum each operator contributes to the shared band. Considering operator selfishness, spectrum sharing based on a non-cooperative game approach can be used to determine the amount of spectrum each operator contributes to the shared band. However, the limited information available to each sharing entity might lead to an unstable sharing scheme. One may consider spectrum sharing for more than two operators enabling inter-operator D2D communication. One could study whether it is beneficial to construct a common pool of spectral resources (see Figure 4.2(a)) or to realize inter-operator D2D by means of bilateral agreements between operators (see Figure 4.2(b)).

In Publications V and VI, overlay inter-operator D2D is considered, where the operators form a spectrum pool by committing spectrum resources dedicated for inter-operator D2D communication, and we study how much spectrum each operator should commit for the spectrum sharing between two operators in Publication V and among more than two operators in Publication VI. While the overlay approach is only considered for intra-operator D2D in Publication V, intra-operator D2D communication might be either in overlay or underlay in Publication VI where no

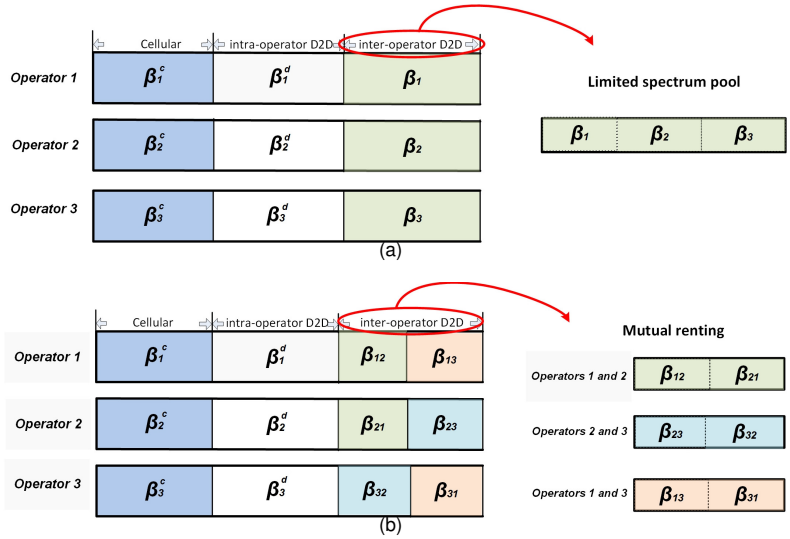

Figure 4.2. (a) Limited spectrum pool and (b) mutual renting in overlay inter-operator D2D.

matter which scheme is used for intra-D2D communication, an operator contributes a fraction of spectrum to the spectrum pool. In Publication IV, overlay intra-operator D2D is considered for a single operator case.

4.2.2 Communication mode

The communication mode is selected by mode selection algorithms which utilize distance, channel quality of cellular and D2D links and interference as selection criteria. In distance-based mode selections, the mutual distance of D2D links [95], and/or the distances between the D2D transmitter and the cellular BS [96] are taken into account. In that case, a D2D transmitter can generate harmful interference to another D2D pair due to the ad-hoc nature of D2D communication where D2D pairs can be arbitrary close to each other. Channel quality-based mode selections are considered in [85, 87, 97, 98]. While a rather simple scenario is considered in [85, 97] with only one D2D pair and one cellular link, multiple D2D pairs are considered in [87, 98] but the optimal selection procedure generates a high amount of signaling overhead, which makes implementation in real networks questionable.

In Publication IV, mode selection according to interference among D2D pairs is proposed, where D2D users could measure the activity in the D2D spectrum, and use a threshold-based test to decide their mode in a distributed way and thus the signaling overhead is minimized. Selection of

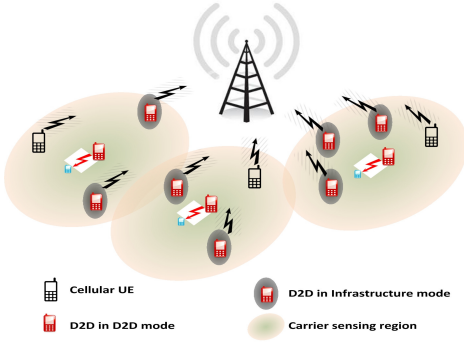

Figure 4.3. Illustration of the mode selection algorithm.

the threshold impacts on the density of D2D pairs and the interference among them. As a result, the optimal threshold is found. When the measured energy is below the threshold, there is indication that there are not many ongoing D2D communications close-by and D2D mode is selected. Otherwise, infrastructure-based mode is selected. The proposed model is also introduced in [80] as an example of distributed mode selection. For the interference-based mode selection, the D2D transmitters employ CSMA-type contention resolution to transmit in D2D mode. The distribution of the transmitters is modeled by the MPP where the hardcore distance δ models the CS range. In Figure 4.3, one can see that potential D2D users inside the CS range of an ongoing D2D communication resort to infrastructure-based mode. In general, the pairwise distance r_d of a D2D pair using a proximity-based service is assumed to be small enough so that the pairwise distance is less than the CS range $r_d < \delta$ which enables use of the MPP model.

4.3 System model

We consider multi-operators enabling D2D communication. Each operator has three types of users: cellular users, intra-operator D2D users, and inter-operator D2D (also referred to as cross D2D) users (see Figure 4.4). Each operator should experience performance gain quantified by excess utility. Taking into account the different types of users, the utility can be expressed as $U_i = U_i(Q_i^c, Q_i^d, Q_i^s)$ where Q_i^k is the average rate of the k-th user type where $k \in \{c, d, s\}$, and c, d and s correspond to cellular, intra-operator D2D and inter-operator D2D users. The function $U_i(\cdot)$ can take different forms, e.g., weighted sum function: $\sum_k w_i^k Q_i^k$, weighted

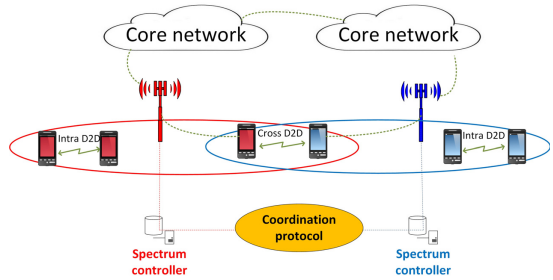

Figure 4.4. User registered to different MNOs communicating in a D2D manner.

max-min function: $\min\{w_i^k Q_i^k \ \forall k\}$, or weighted proportional fair function: $\sum_k w_i^k \log Q_i^k$ where $w_i^k \geq 0$ are weights indicating the normalized densities of different types of users. In this chapter, we assume that each operator considers the average D2D user rate, expressed as

$$U_i = (1 - w_i^s)\, Q_i^d + w_i^s\, Q_i^s, \quad i \in \{1, \cdots, K\} \tag{4.1}$$

where K is the number of operators.

The average rate of each type of user is associated with link spectral efficiency in equation (2.4), user density fraction and available bandwidth. In a real system, the spectral efficiencies can be computed based on the measurements. In this chapter, in order to capture the behavior of the system which is described by distributions, we use a stochastic geometry approach (see Chapter 2) where the locations of BS, cellular, intra-operator and inter-operator D2D users follow independent PPPs with densities, λ_i^b, λ_i^c, λ_i^d and $\lambda = \sum_i \lambda_i$ where λ_i is the density of the inter-operator D2D transmitters for i-th operator, respectively. For the inter-operator D2D pairs, we assume that the densities of the transmitters from different operators are equal, $\lambda_i = \lambda/K, \forall i$. The BSs form a Voronoi tessellation and cellular users communicate with their nearest BS (also referred to as home BS). In this chapter, we do not incorporate power control into our analysis neither for cellular nor for D2D users.

4.4 Interference model

In the overlay intra-operator and overlay inter-operator D2D schemes, there are no cross-tier interference issues among users operating in cellular mode and D2D modes for intra-operator and inter-operator D2D communications. However, there is still self-interference generated from

users in each communication mode.

4.4.1 Interference in cellular mode

With in-band D2D overlay mode, the interferers in cellular mode are cellular transmitters from other cells, i.e., cellular users and intra-operator and inter-operator D2D users operating in cellular mode. Mode selection allows a D2D user to transmit in intra-operator D2D mode with probability q_i^d and in inter-operator D2D mode with probability q.

Thus, all users operating in cellular mode for an operator would generate in the uplink mean interference equal to the mean interference from a PPP $\Phi_i^{CM,a}$ with density $\lambda_i^c + (1-q_i^d)\lambda_i^d + (1-q)\lambda/K$. In the uplink of a cellular system with round-robin scheduling, only one transmitter is active in a cell at any particular moment. Scheduling introduces dependency in the process $\Phi_i^{CM,a}$. To simplify the analysis we assume that the locations of cellular interferers form a PPP Φ_i^{CM} with density λ_i^b [95].

The interference at the typical BS is given by $I_i^{CM} = \sum_{k\in\Phi_i^{CM}\setminus o} P \cdot x_k \cdot l(r_k)$ where x_k describes the fading from the k-th interferer following exponential distribution with mean equal to unity. In the presence of Rayleigh fading, the distribution of the random variable I_i^{CM} is characterized in terms of LT which is given by

$$\mathcal{L}_{I_i^{CM}}(s) = E_o^!\left[e^{-s\cdot I_i^{CM}}\right] = E_o^!\left[e^{-s\cdot\sum_{k\in\Phi_i^{CM}} P\cdot x_k\cdot l(r_k)}\right] \tag{4.2i}$$

$$\overset{(p1)}{=} E_o^!\left[\prod_{k\in\Phi_i^{CM}} e^{-s\cdot P\cdot x_k\cdot l(r_k)}\right] \overset{(p2)}{=} E_o^!\left[\prod_{k\in\Phi_i^{CM}} \frac{1}{1+\frac{\gamma_t\cdot l(r_k)}{l(r_c)}}\right] \tag{4.2ii}$$

$$\overset{(p3)}{=} e^{-2\pi\cdot\kappa\cdot\lambda_i^{bs}\cdot\int_{r_c}^{\infty}\frac{\gamma_t\cdot l(r_k)/l(r_c)}{1+\gamma_t\cdot l(r_k)/l(r_c)}\cdot r_k\cdot dr_k} = e^{-2\pi\cdot\kappa\cdot\lambda_i^{bs}\cdot\frac{r_c^2\cdot\gamma_t}{\alpha-2}\,{}_2F_1\left(1,\frac{\alpha-2}{\alpha},2-\frac{2}{\alpha},-\gamma_t\right)} \tag{4.2iii}$$

where $E_o^![\cdot]$ is the expectation with respect to the reduced Palm measure [20], $(p1)$ follows from the i.i.d. distribution of the fading x_k, $(p2)$ follows from the exponential distribution of x_k with mean equal to unity, $(p3)$ follows from the conditional PGFL [37] which is equal to the PGFL of the PPP by Slivnyak's theorem, expressed as $E_o^![\prod_{t\in\phi} f(t)] = e^{-\lambda\int_{\mathcal{R}^n}(1-f(t))dt}$, r_c is the distance of a cellular user to its nearest BS, and κ is the probability a BS is active.

4.4.2 Interference in D2D mode

The upper bound for the interference in contention-based networks is useful for different reasons. While an upper bound for the mean interference at the receiver can be used to ensure that a target outage probability is satisfied, the one at a transmitter can be useful for ensuring the target performance in cellular mode. This is because introducing D2D communication should not degrade the performance of a cellular system.

The set of D2D users scheduled in intra-operator D2D mode Φ_i^{DM} and inter-operator D2D mode $\Phi^{DM'}$ can be obtained by thinning the parent PPPs with respective hardcore distance, and the densities of transmissions in each D2D mode are $q_i^d\lambda_i^d$ and $q\lambda$. The mean interference at a typical D2D transmitter in D2D mode, given by $I_{i,tx}^{DM} = \sum_{k\in\Phi_i^{DM}\setminus o} P\cdot x_k\cdot l(r_{k,t})$ in intra-operator D2D mode and by $I_{i,tx}^{DM'} = \sum_{k\in\Phi_i^{DM'}\setminus o} P\cdot x_k\cdot l(r_{k,t})$ in inter-operator D2D mode, can be set equal to the CS threshold for controlling the density of respective D2D mode transmissions. Note that an upper bound for the CS threshold will result in less D2D users allocated in the cellular spectrum and thus, it favors the QoS of cellular users. In this regard, we obtain the following upper bound for the CS threshold

$$E_o^!\left[I_{i,tx}^{DM}\right] = E_o^!\left[I_{i,tx_{<2\delta}}^{DM}\right] + E_o^!\left[I_{i,tx_{>2\delta}}^{DM}\right] \tag{4.3i}$$

$$\leq 2\pi q_i^d\lambda_i^d\int_{\delta}^{2\delta} l(r)\overline{g}(r)dr + 2\pi q_i^d\lambda_i^d\int_{2\delta}^{\infty} l(r)dr \tag{4.3ii}$$

using the upper bound $\overline{g}(r)$ for the PCF $g(r)$ of MPP type II with given HCD δ. The mean interference at a typical transmitter in inter-operator D2D mode can be expressed in a form similar to equation (4.3) after replacing $I_{i,tx}^{DM}$ with $I_{i,tx}^{DM'}$ and $q_i^d\lambda_i^d$ with $q\lambda$.

The interference at the typical D2D receiver in D2D mode is given by in intra-operator D2D mode, $I_i^{DM} = \sum_{k\in\Phi_i^{DM}\setminus o} P\cdot x_k\cdot l(r_k)$, and, in inter-operator D2D mode, $I_i^{DM'} = \sum_{k\in\Phi_i^{DM'}\setminus o} P\cdot x_k\cdot l(r_k)$. The distribution of the random variable I_i^{DM} is characterized in terms of LT which is given by

$$\mathcal{L}_{I_i^{DM}}(s) = E_o^!\left[e^{-s\cdot I_i^{DM}}\right] = E_o^!\left[e^{-s\cdot\sum_{k\in\Phi_i^{DM}} P\cdot x_k\cdot l(r_k)}\right] \tag{4.4i}$$

$$= E_o^!\left[\prod_{k\in\Phi_i^{DM}} e^{-s\cdot P\cdot x_k\cdot l(r_k)}\right] = E_o^!\left[\prod_{k\in\Phi_i^{DM}}\frac{1}{1+\frac{\gamma_t l(r_k)}{l(r_d)}}\right] \tag{4.4ii}$$

Note that the PGFL of MPP type II is not known. One way to resolve the

issue is presented in [30] to take an approximation on the complementary outage probability by using Weierstrass inequality [99]. However, their proposed bounds are valid for very small D2D user densities λ_i^d and a low SINR target γ_t. As an alternative approach, we take an approximation for the PGFL of MPP type II to obtain an approximation on the interference distribution, which is similar to the approximation on the complementary outage probability by using Jensen's inequality [31], but more reliable and simple.

For the approximation on the interference distribution, based on the fact that the mean interference received from the correlated area S_2^d of an MPP type II process (see Chapter 2) where $S_2^d = \{(r,\phi) : 0 \leq \phi \leq 2\pi, \delta < r < 2\delta\}$ can be upper bounded by a PPP with density $cq_i^d\lambda_i^d$ where the constant $c = 2\pi/(4\pi/3+\sqrt{3}/2)$, we make the assumption that the PGFL of an MPP type II in the area S_2^d can be lower bounded by the PGFL of a PPP with density $cq_i^d\lambda_i^d$ and as a result, we obtain the approximated LT for equation (4.4)

$$\mathcal{L}_{I_i^{DM}}(s) \approx E_o^! \left[\prod_{k \in \Phi_i^{DM}(S_1^d)} \frac{1}{1+\frac{\gamma_t \cdot l(r_k)}{l(r_d)}} \right] \cdot E_o^! \left[\prod_{k \in \Phi_i^{DM}(S_2^d)} \frac{1}{1+\frac{\gamma_t \cdot l(r_k)}{l(r_d)}} \right] \tag{4.5i}$$

$$\approx e^{-q_i^d\lambda_i^d \int_0^{2\pi}\int_{2\delta}^{\infty} \frac{\gamma_t \cdot l(r_k)/l(r_d)}{1+\gamma_t \cdot l(r_k)/l(r_d)} \cdot r \cdot dr \cdot d\phi - cq_i^d\lambda_i^d \int_0^{2\pi}\int_{\delta}^{2\delta} \frac{\gamma_t \cdot l(r_k)/l(r_d)}{1+\gamma_t \cdot l(r_k)/l(r_d)} \cdot r \cdot dr \cdot d\phi} \tag{4.5ii}$$

where $S_1^d = \{(r,\phi) : 0 \leq \phi \leq 2\pi, r \geq 2\delta\}$, r_d is the pairwise distance of a D2D pair, and $r_k = \sqrt{r^2 + {r_d}^2 - 2 \cdot r \cdot r_d \cdot \cos\phi}$ is the distance between the typical D2D receiver and its k-th D2D interferer in D2D mode. The LT for the aggregate interference distribution in inter-operator D2D mode can be expressed in a form similar to equation (4.5) after replacing I_i^{DM} with $I^{DM'}$, Φ_i^{DM} with $\Phi^{DM'}$, and $q_i^d\lambda_i^d$ with $q\lambda$. The expressions for the LT in equations (4.4) and (4.5) can be used to derive the coverage probability of a cellular uplink and D2D link in the presence of Rayleigh fading (See section 2.1.2).

4.5 Interference control and spectrum allocation

In D2D overlay mode, self-interference in D2D mode can be controlled by mode selection which tunes a common CS threshold among D2D transmitters. Selecting a CS threshold would determine the number of D2D users operating in D2D mode and in cellular mode. This implies that the CS threshold in mode selection would affect the performance in D2D

mode as well as in cellular mode, i.e., lower CS threshold decreases self-interference for a D2D link and the time resource for a cellular uplink.

To overcome the low flexibility and low spectrum utilization problem suffering from exclusive usage in the overlay approach, a combination of exclusive spectrum allocation and proper mode selection algorithm is needed. Efficient spectrum allocation is based on the constrained optimization problem such as the operator-specific objective shown in equation (4.1) and operator-specific constraint shown later. The problem is related to the performance evaluated in cellular mode and D2D mode.

Given the densities of the D2D users, BSs and cellular users, a network management entity should divide the spectrum between D2D and infrastructure communication and also set the CS threshold for the D2D users. These values are then broadcasted from the BSs to the D2D users.

4.5.1 Mode selection and spectrum allocation for an operator

The CS threshold and the spectrum partition factor can be selected to maximize various optimization criteria of the cellular system. We set the optimization parameters for maximizing the rate of the intra-operator D2D users by setting $w_i^s = 0$ in equation (4.1), under some constraint on the average rate of cellular users Q_i^c larger than a target value τ

$$\begin{aligned} \underset{\beta=\beta_i^d}{\text{Maximize}}: \quad & Q_i^d. \\ \text{Subject to}: \quad & Q_i^c \geq \tau \end{aligned} \tag{4.6}$$

The average rate of cellular users Q_i^c is equal to the spectral efficiency of links in cellular mode multiplied by the available bandwidth $(1 - \beta)$. On the other hand, the average rate of intra-operator D2D users Q_i^d is obtained as an average of the spectral efficiency of links in intra-operator D2D mode and cellular mode, scaled with the normalized user density and transmission bandwidth, respectively. The spectral efficiencies in the presence of Rayleigh fading can be expressed as the LT expression of the aggregate interference, obtained by putting equations (4.2) and (4.5) in equation (2.4).

Less allocated spectrum in cellular mode can be compensated by a higher CS threshold increasing the density of users in D2D mode and making enough time resources available for cellular communication. Thus, spectrum allocation and mode selection needs to be considered simultaneously for efficient spectrum sharing, i.e., allocating more spec-

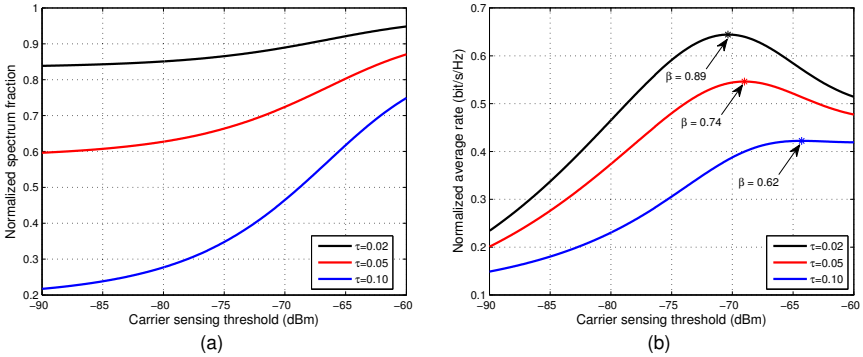

Figure 4.5. (a) feasibility region, i.e., CS thresholds and spectrum allocation factors for intra-operator D2D mode given the target rate for cellular mode and (b) normalized average rate for intra-operator D2D users, when $\lambda_i^d = 10 \cdot \lambda_i^b$.

trum for D2D mode should be combined with a higher CS threshold (see Figure 4.5(a)).

For a low threshold, the interference among D2D users is low but the associated bandwidth is low too, which results in the low overall D2D rate. However, increasing the allocated bandwidth beyond a certain point has adverse effects. Due to the associated high CS threshold, the D2D self-interference starts reducing the rate in D2D mode. This yields an optimal point, i.e., the spectrum partition factor and CS threshold where the D2D user rate is maximized (see Figure 4.5(b)).

In spectrum sharing for D2D communication, there should be at least a positive sum rate gain achieved by a cellular system enabling D2D communication in comparison with a conventional cellular system where all transmissions use the BS as a relay. For high D2D user density, the gain decreases, since the spectrum allocation factor β decreases to satisfy the cellular target rate τ and at the same time the density of users in D2D mode increases. Significant gain can be obtained for all considered D2D user densities due to the overall benefit of localized communication (see Figure 4.6).

4.5.2 Game theory-based spectrum allocation for multiple operators

In this subsection, the goal is to identify how much spectrum each operator should commit for overlay inter-operator D2D communication. Since operators are reluctant to exchange operator-specific information, i.e., utility function and channel state, the inter-operator spectrum sharing has been considered as a game where operators participating in the game

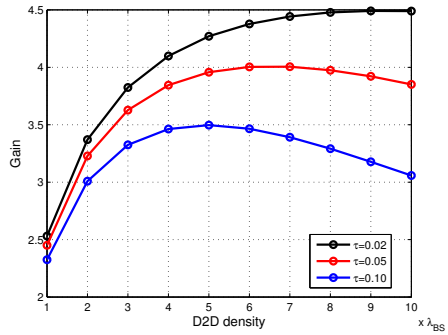

Figure 4.6. Gain in comparison with a cellular system without D2D mode functionality, expressed as $\frac{\lambda_i^c \cdot Q_i^c + \lambda_i^d \cdot Q_i^d}{(\lambda_i^c + \lambda_i^d) \cdot R_i^c}$

are players and can compete to maximize their utility. For this, we formulate a non-cooperative spectrum sharing game where the operators make offers about the amount of spectrum they want to contribute to a spectrum pool, in a parallel manner, and we design an iterative algorithm to reach a consensus.

The uniqueness of the Nash Equilibrium (NE) is critical for predicting the outcome of a game. In case there are multiple NEs, the selected equilibrium would depend on the initial strategy profile [100]. This might be undesirable because the performance of an operator would depend on the initial proposals of other operators. The stability of a NE depends on the general strategy adjustment process. Each operator iteratively adjusts its strategy profile in response to the adjustment made by others. If the NE obtained as a result of such iterative play is globally stable, no matter where the game starts the final outcome is the same, the global stability of equilibrium candidate points implies uniqueness. In Publication VI, some conditions under which each operator identifies the uniqueness of the NE in a distributed manner and can stably converge to the NE, are provided.

In a non-cooperative game, each player sets its strategy profile to maximize the utility in equation (4.1), under operator-specific constraints for cellular users Q_i^c and intra-operator D2D users Q_i^d larger than the target values μ_i and τ_i respectively

$$\underset{\beta_i \geq \beta_i^{min}}{\text{Maximize}}: \quad U_i \tag{4.7a}$$

$$\text{Subject to}: \quad Q_i^c \geq \mu_i \tag{4.7b}$$

$$Q_i^d \geq \tau_i \tag{4.7c}$$

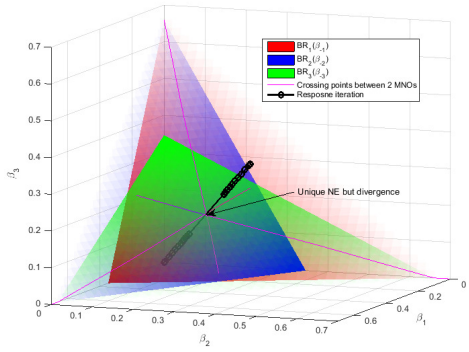

Figure 4.7. Illustration of NE divergence of best-reply, $BR_i(\cdot), i \in \{1, \cdots, N\}$ for $N = 3$ MNOs (Mobile Network Operators). Shaded area shows best-reply strategy profiles responding to opponents' aggregate proposal, β_{-i}: $\beta_i = BR_i(\beta_{-i})$. There exists a unique NE at crossing point but the iterative best-reply process (Black line) diverges.

Conditions to have a unique NE point can be identified, when every operator has a concave utility function in equation (4.1) $\frac{\partial^2 U_i}{\partial \beta_i^2} < 0$ in the box-constrained region $\beta_i^{min} \leq \beta_i \leq \beta_i^{max}$. Since the objective in (4.7a) is concave and the constraints in (4.7b) and (4.7c) are decreasing with respect to β_i, the optimization problem (4.7) can be transformed into an equivalent one of maximizing a concave utility subject to a box constraint.

Due to the lack of knowledge of other player's condition, the iterative process may not converge to the desired operating point. Two different iterative algorithms, best-reply and jacobi-play strategy updates, can be considered for stably converging to the unique NE. Even if there is a unique NE, the best-reply might not converge to the equilibrium point due to myopically overreacting to the responses of the other operators (see Figure 4.7). On the other hand, the jacobi-play strategy update algorithm can converge with an appropriate selection of update parameter [101].

Using the jacobi-play update algorithm, we illustrate that the asymmetric operators who have different intra-operator D2D densities would contribute unequal amounts of spectrum (see Figure 4.8(a)) but all experience performance gain compared to the case without inter-operator D2D support (see Figure 4.8(b)). For densities $\lambda_1^d < 5$, operator 1 who has less network load contributes the higher fraction of spectrum in the spectrum pool, since it has enough capacity to satisfy its own rate constraints. Because of that, the other operators enjoy more benefit from spectrum sharing than the operator 1 does. On the other hand, for densities $\lambda_1^d > 5$, operator 1 contributes only a small fraction for the signaling channel. Op-

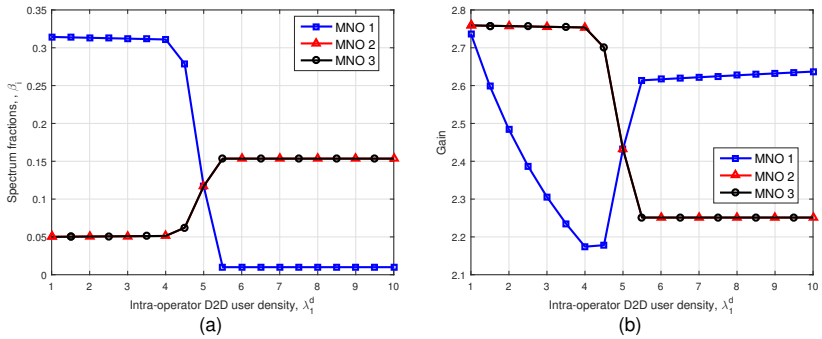

Figure 4.8. (a) Spectrum fraction, β_i, for inter-operator D2D, w.r.t density of D2D users for the operator 1, λ_1^d, and (b) Gain for the operators as compared to the case without co-primary spectrum sharing, w.r.t density of D2D users for the operator 1, λ_1^d, when $N{=}3$ and $\lambda_{i\geq 2}^d = 5$.

erator 2 and operator 3 still benefit by contributing more fraction. The performance gain for all operators is high, only if the network load for operator 1 becomes low.

4.6 Discussion

In this chapter, we discussed mechanisms for mode selection and radio spectrum allocation for overlay D2D communication. A potential D2D user measures the activity over the spectrum allocated for D2D transmissions and uses a CS threshold to decide about its transmission mode. By appropriately selecting the CS threshold, the interference among D2D communication pairs can be controlled and their performance can be improved. This distributed nature of this mechanism leads to less signaling overhead between D2D users and BSs even in dense deployments. Based on this method, we find spectrum allocation factors and CS thresholds for maximizing the rate of D2D users under the target rate constraint for cellular users. Note that while the mode selection is based on the CCA at the corresponding transmitter, a more efficient mode selection algorithm would be possible by an additional sensing operation at the desired receiver. In the modified version of SSI, the receiver is involved in the selection process [71], but its temporal process suffers from mathematical intractability. Since D2D communications are usually within a short distance, and thus a D2D pair experiences similar channel propagation property, the proposed algorithm would be still a feasible solution for distributed mode selection.

In the multi-operator D2D setting, the operators may not be willing

to reveal proprietary information to the competitor and/or to other parties. Because of that, we modeled their interaction as a non-cooperative game. An operator makes an offer about the amount of spectrum to contribute for multi-operator D2D communication considering only its individual performance. In Publication VI, an iterative algorithm based on a jacobi-play update is designed with a careful selection of update parameter for a spectrum sharing scenario where a general number of operators construct a spectrum pool dedicated to support inter-operator D2D communication. The formulated game has a unique NE and the sequence generated by the iterative algorithm converges to it from any initial point. Using the proposed spectrum sharing solution, we illustrate that all operators may experience significant performance gains as compared to no spectrum sharing. In general, asymmetric operators contribute unequal amounts of spectrum. An operator may not contribute any spectrum at all. Nevertheless, the opponent may have the incentive to be cooperative due to the D2D proximity gain. Operators may experience significant performance gains. The particular gain would depend on the operator-specific network load, utility and design constraints.

Note that the NE is generally not Pareto-efficient [102], while solutions at NE points can be obtained by several distributed algorithms. Comparison of NE with Pareto optimality is studied in [103]. It is shown that Pareto-optimal solutions can be achieved as an NE of the game in selfish but cooperating systems. The cooperative approach has a significant increase of signaling overhead and coordination among the operators.

Note that the consequence of the myopic manner in the iterative parallel and distributed algorithm might result in a slow convergence rate and thus might cause a real-time implementation problem. To resolve this issue, different sequential algorithms such as round robin or random polling have been proposed in [104] for a dynamic non-cooperative game. However, their convergence analysis is only valid for the linearized version of best-reply algorithm.

5. Vehicle-mounted base stations in femto base stations

In this chapter, we consider spectrum sharing across two-tier heterogeneous small-cell networks between outdoor and indoor small-cells in a dense urban city environment, i.e., for frequency planning between street microcells and indoor femtocells, and focus on the problems of the inter-cell interference generated from outdoor users along urban street microcells towards indoor femtocell users.

5.1 Introduction

The concept of vehicle-mounted BSs (also referred as moving/parked car BSs or relays) has been developed to support multi-tier heterogeneous networks with macrocells or microcells [105–107]. Such coexistence of heterogeneous networks within the same spectrum is a promising method to enhance the spectrum efficiency. Further network densification along urban street microcells can be used to increase the amount of served load. At the same time, passengers inside a vehicle can connect to a micro BS through a gateway with an antenna mounted on the roof of the vehicle overcoming high penetration loss [108], thereby improving the performance for users in the vehicle [109, 110]. However, the road to success is filled with challenges such as spectrum authorization and associated interference issues.

For the spectrum authorization scheme for vehicle-mounted BSs, one option could be to either partition the spectrum between the macro and the micro layers, or use the full spectrum under a shared spectrum access regime. A similar approach has been proposed for overlaying indoor femtocells on macrocells [111]. Wireless data traffic offloading to indoor-femto cellular band can be considered as a solution for a vehicle-mounted BS in an outside urban area. Such spectrum coexistence between two

small-cells in the micro and the femto layers could lead to high spectral efficiency. However, the aggregate cross-tier interference generated from the high densed vehicle-mounted BSs to the femtocells would form the main performance bottleneck in a dense urban area [112, 113].

Most of the existing studies [114–116] related to vehicle-mounted BSs either deal with system architecture issues or study the performance of vehicle-mounted BSs in simplified scenarios, without considering practical challenges in ultra-dense urban scenarios. In typical outdoor urban scenarios, due to the densely deployed small-cells and street canyon effects, practically it might be more complicated inter-cell interference. To address this issue, the performance of a vehicle-mounted BS in the Madrid grid model with a heterogeneous deployment of macro and micro BSs is evaluated in [117]. However, coexistence between microcell and femtocell is not studied, and no mathematical tractability is provided.

In this chapter, we present the main methods and results of Publication VII, aiming to study spectrum coexistence issues between the micro and femto layers. In order to answer the question: whether the vehicle-mounted BSs could coexist with an indoor femtocell network or not, we assess the impact of outdoor vehicular transmissions in microcells along urban streets on indoor users. To this aim, we develop a model for aggregate interference distribution and SIR distribution at the worst case indoor femtocells. The proposed model enables a dynamic evaluation of outage probability in coordination mechanisms between the involved co-primary small-cell networks. And this model can be used by a spectrum allocation database evaluating the performance at the femtocell and deciding whether to allocate vehicular and femtocell transmissions in the same spectrum under a given density of vehicles. The model is presented in the TeC08 of METIS deliverable D5.4 [9]. The details of the analysis and more results can be found in Publication VII.

5.2 System model

We consider an abstract and simplified deployment model as shown in Figure 5.1 for a dense urban city [118, TC2]. In order to study whether vehicle communication and indoor femtocells can coexist in the same spectrum or not, we focus on the performance at the worst case femtocell limited by the interference level. The outage probability for the given SIR

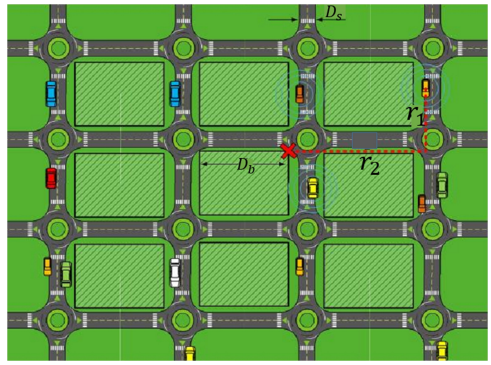

Figure 5.1. System illustration.

target γ_t at the worst-case located femtocell facing a cross road is

$$O_t = \Pr[\text{SIR} < \gamma_t] \tag{5.1}$$

characterized by the SIR distribution which depends on the useful signal distribution and the aggregate interference distribution at the femtocell.

There are two interfering links to the femtocell: a backhaul link between an antenna on the roof of the vehicle and a street microcell, and an access link between in-vehicle BS and the users inside the vehicle. The backhaul and access links operate at different frequency bands as in full-duplex fashion. For the two links, two spectrum sharing scenarios are considered. The spectrum of indoor femtocell is shared either i) with the backhaul link, i.e., antenna on the roof of the vehicle generates interference to the indoor cell, or ii) with the access link, i.e., in-vehicle communication generates interference to the indoor cell. The impact of two links to the femtocell is differentiated by vehicle isolation η, generating different channel gain, when the same transmitting power is used for the two links.

Along a street, the active vehicles are distributed according to one dimensional PPP on the j-th vertical street by Φ_j^{VU} with density λ_j^{vu} and on the j'-th horizontal street by $\Phi_{j'}^{VU}$ with density $\lambda_{j'}^{vu}$. Both streets in the Manhattan two-dimensional grid are symmetric and a constant vehicle density is used on all the streets. The independent property of PPP allows us to focus only on one type of street and incorporate the impact of horizontal streets. In [119], one-dimensional PPP is used to model the locations of vehicles in two perpendicular single-lane roads, but the canyon effect is ignored in their analysis.

While the power law model is sufficient to describe distance-based propagation pathloss in outdoor macrocells, attenuation along street microcells is described by more accurate models where the power law changes beyond a certain distance breakpoint [120]. The distance-based pathloss in the Manhattan grid $l(r_1, r_2) = Cr_1^{-2}r_2^{-\alpha}$ is a function of attenuation constant C, NLOS distance r_1, LOS distance r_2, and the attenuation exponent α (see also Figure 5.1). The impact of fast/slow fading can also be incorporated into the model. This model captures the main characteristics of practical pathloss, but it is much simpler to analyze than, e.g., Urban Micro (UMi) models [121], and thus makes the analytic treatment of interference distribution more involved with a stochastic geometry approach. We assume that the source-destination fading is Nakagami-m distributed and the interfering fading is Rayleigh distributed. Next, we propose a model for the interference distribution and evaluate its moments.

5.3 Interference model

In this section, we aim to model the aggregate interference generated from a vehicle-mounted BS at an indoor femtocell user located at the building corner near the street intersection. The aggregate interference comes from the concurrent transmitting vehicle-mounted BSs on all streets utilizing the femtocell channel. The amount of interference generated to the femtocell user at the worst location, i.e., the building corner, can be expressed as the sum of interference levels from all active vehicle BSs on all vertical and horizontal streets

$$\begin{aligned} I^{VU} &= \sum_{j} I_j^{VU} + \sum_{j'} I_{j'}^{VU} \\ &= \sum_{j} \sum_{k \in \Phi_j^{VU}} P \cdot x_k \cdot l(r_{1,k}, r_{2,j}) + \sum_{j'} \sum_{k' \in \Phi_{j'}^{VU}} P \cdot x_{k'} \cdot l(r_{1,k'}, r_{2,j'}) \end{aligned} \tag{5.2}$$

The aggregate interference can be completely characterized by its PDF, but there is no known expression for the PDF of the interference I^{VU} in (5.2). Thus, alternatively, the aggregate interference can be characterized by using the LT of the interference distribution. When the integral for the inverse LT does not exist in closed-form, the use of approximations for the aggregate interference is motivated as a means to provide simple and useful expressions. Next, we show 1) the LT of the interference distribution by using the property of PPP, e.g., the PGFL, and 2) the approxi-

mated interference by using the method of moments, which estimates the parameters of interest.

5.3.1 Laplace Transform of interference distribution

The LT of the aggregate interference from vehicles distributed as one-dimensional PPP on the j-th vertical street in a Manhattan grid is given by

$$\mathcal{L}_{I_j^{VU}}(s) = E\left[e^{-s\cdot I_j^{VU}}\right] = E\left[e^{-s\cdot\sum_{k\in\Phi_j^{VU}} P\cdot x_k\cdot l(r_{1,k},r_{2,j})}\right] \tag{5.3i}$$

$$\overset{(p1)}{=} E\left[\prod_{k\in\Phi_j^{VU}} e^{-s\cdot P\cdot x_k\cdot l(r_{1,k},r_{2,j})}\right] \overset{(p2)}{=} E\left[\prod_{k\in\Phi_j^{VU}} \frac{1}{1+sPx_k l(r_{1,k},r_{2,j})}\right] \tag{5.3ii}$$

$$\overset{(p3)}{=} e^{-2\lambda_j^{vu}\int_0^\infty \frac{s\cdot P\cdot l(r,r_{2,j})}{1+s\cdot P\cdot l(r,r_{2,j})}dr} = e^{-\pi\lambda_j^{vu}\sqrt{\frac{s\cdot P\cdot C}{(j\cdot D)^\alpha}}} \tag{5.3iii}$$

where $(p1)$ follows from the i.i.d. distribution of the fading x_k, $(p2)$ follows from the exponential distribution of x_k with mean equal to unity, and $(p3)$ follows from the PGFL [37] of the one-dimensional PPP.

Since the PPPs along different vertical streets are independent among each other, the LT of the aggregate interference from all vertical streets $\mathcal{L}_{I^{VU}}(s)$ is equal to the product of the LTs from each vertical street [122]

$$\mathcal{L}_{I^{VU}}(s) = \prod_j \mathcal{L}_{I_j^{VU}}(s) = e^{-\pi\lambda^{vu}\left\{1+\zeta\left(\frac{\alpha}{2}\right)D^{-\frac{\alpha}{2}}\right\}\sqrt{s\cdot P\cdot C}} \tag{5.4}$$

where $\zeta(\cdot)$ denotes the Riemann zeta function, $D = D_b + D_s$ is the distance between neighboring streets in Figure 5.1, $z = P\cdot C$ for singular pathloss model, and $\lambda^{vu} = \lambda_j^{vu}, \forall j$.

The singular pathloss model might cause inaccurate interference modeling in the near-field, i.e., infinite interference level when $r_1 = 0$ and $r_{2,j} = 0$. In a more practical case, a non-singular pathloss model is taken into account by limiting $r_1 \geq 1$, and $r_{2,j} = 1$ is considered for the vertical street facing the considered femtocell $j = 0$. Thus, the LT of the aggregate interference from the j-th street is

$$\mathcal{L}_{I_j^{VU}}(s) = e^{-2\lambda_j^{vu}\int_1^\infty \frac{s\cdot P\cdot l(r,r_{2,j})}{1+s\cdot P\cdot l(r,r_{2,j})}dr} = e^{-2\lambda_j^{vu}\int_1^\infty \frac{s\cdot P\cdot C}{(j\cdot D)^\alpha r^2+s\cdot P\cdot C}dr} \tag{5.5i}$$

$$\overset{(p1)}{=} e^{-2\lambda_j^{vu}\sqrt{\frac{s\cdot P\cdot C}{(j\cdot D)^\alpha}}\arctan\left(\sqrt{\frac{s\cdot P\cdot C}{(j\cdot D)^\alpha}}\right)} \tag{5.5ii}$$

where (p1) follows from the integration rule $\int_1^\infty \frac{s}{ur^2+s}dr = \sqrt{\frac{s}{u}}\cdot\arctan(\sqrt{\frac{s}{u}})$

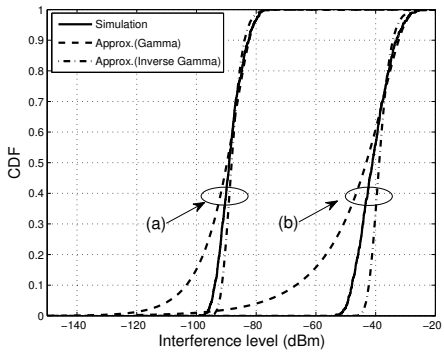

Figure 5.2. Approximations of interference level distribution using Gamma and inverse-Gamma distribution with non-singular pathloss model, when (a) the interference from the closest street $j = 0$ is not considered and (b) the interference from all vertical streets is considered.

[123, 2.172], and the one from all vertical streets is

$$\mathcal{L}_{I^{VU}}(s) \quad = \quad e^{-2\lambda^{vu}\sum_{j=0}^{\infty}\sqrt{\frac{s\cdot P\cdot C}{(j\cdot D)^{\alpha}}}\arctan\left(\sqrt{\frac{s\cdot P\cdot C}{(j\cdot D)^{\alpha}}}\right)} \tag{5.6}$$

5.3.2 Approximation of interference distribution

The interference is approximated by using inverse Gamma distribution and Gamma distribution with second-order moment matching, based on the fact that the LT of the interference in equation (5.4) resembles the CF of the Levy distribution. With Method #1 in section 2.1.1, the interference distribution is approximated by a fitted inverse Gamma distribution with scale $a = \frac{\mathbf{E}[I^{VU}]^2}{E[I^{VU\,2}]-\mathbf{E}[I^{VU}]^2} + 2$ and shape $b = E[I^{VU}](a-1)$ and Gamma distribution with scale a and shape $1/b$, $I^{VU^{-1}} \sim g_{a,1/b}$. The first two moments of the interference can be found based on the LT, $E[I^{VU^n}] = \lim_{s\to 0}(-1)^n \frac{d^n}{ds^n}\mathcal{L}_{I^{VU}}(s)$ and expressed as

$$E[I^{VU}]=2\lambda^{vu}\sum_{j=0}^{\infty}\frac{z}{(j\cdot D)^{\alpha}}=2\lambda^{vu}\cdot z\left(1+\frac{\zeta(\alpha)}{D^{\alpha}}\right) \tag{5.7i}$$

$$E[I^{VU\,2}]=\frac{4\lambda^{vu}}{3}\sum_{j=0}^{\infty}\frac{z^2}{(j\cdot D)^{2\alpha}}+E[I^{VU}]^2=\frac{4\lambda^{vu}\cdot z^2}{3}\left(1+\frac{\zeta(2\alpha)}{D^{2\alpha}}\right)+E[I^{VU}]^2 \tag{5.7ii}$$

Both distributions are accurate in the upper tail which would determine the accuracy of the approximation in the lower tail of the SIR distribution (see Figure 5.2). The inverse Gamma distribution achieves better approximation over the full distribution body. And it is interesting to note

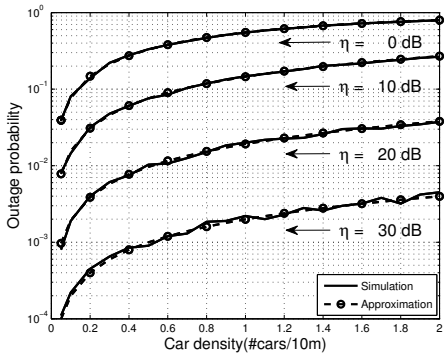

Figure 5.3. Comparison of outage probability for simulation result and analytical result in equation (2.3) with respect to vehicle BS density λ and vehicle isolation η when Nakagami fading parameter $m = 1$, mean wanted signal level is $\overline{W} = -40$ dBm and SIR target is $\gamma = 15$ dB. For mounted roof-top antenna, car isolation is equal to $\eta = 0$ dB.

that the mean interference level decreases by approximately 50 dB if the impact of the street facing the femtocell of interest $j = 0$ is not considered. For mounted roof-top antennas, frequency planning between street microcells and indoor femtocells could be an option for performance enhancement.

5.4 Interference control

With a low complex and accurate interference model, we aim to control some parameters such as the density of vehicles and the uplink transmit power level to control the aggregate interference and to satisfy the outage probability which can be illustrated by 1) the LT of the aggregate interference and 2) by the approximated SIR distribution.

With Method #2 in section 2.1.2, the outage probability, when the source destination fading is Nakagami-m distributed with mean signal level $\overline{W}$, can be expressed in terms of the LT of the aggregate interference. The outage probability at the femtocell is approximated as a function of the density λ^{vu} of uplink transmissions (see Figure 5.3). With more than a 20 dB increase in vehicle isolation or reduction in transmit power level, the outage probability decreases at acceptable values even for a high density of vehicles.

The amount of computations might be high particularly when the shape m of the Nakagami distribution is high (see equation (2.3) in Chapter 2). Approximating the SIR distribution can be useful for estimating not only the outage probability but also the moments of the SIR distribution. This

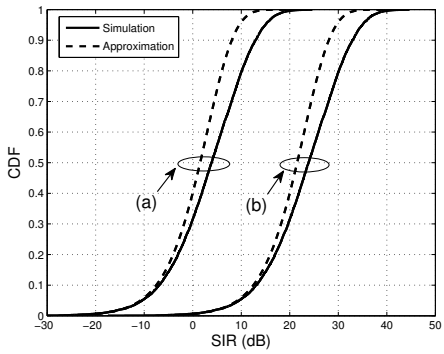

Figure 5.4. SIR distribution when vehicle BS density is $\lambda^{vu} = 0.1$ cars/m, the mean wanted signal level is $\overline{W} = -40$ dBm, and vehicle isolations are (a) $\eta = 0$ dB and (b) $\eta = 20$ dB

fact motivates the use of approximations for the SIR distribution by some known function so as to assess its mean and higher moments in a low-complex manner.

The SIR $W \cdot I^{VU^{-1}}$ can be expressed as product of two independent Gamma random variables, since the useful signal level in the Nakagami-m fading channel is Gamma distributed with scale m and shape θ, $W \sim g_{m,\theta}$ where $\theta = \frac{\overline{W}}{m}$, and the inverse interference level is also Gamma distributed with $I^{VU^{-1}} \sim g_{a,1/b}$. By normalizing the respective shape parameters, the normalized SIR $\gamma_n = \frac{b}{\theta} \cdot \frac{W}{I^{VU}}$ becomes the product of two Gamma random variables with shape equal to unity, $g_1 = W \cdot \theta^{-1} \sim g_{m,1}$ and $g_2 = I^{VU^{-1}} \cdot b \sim g_{a,1}$, thus $\gamma_n = g_1 \cdot g_2$. The resulting PDF of the normalized SIR can be expressed in terms of a Meijer G-function [124]. The corresponding CDF can be obtained by integrating over the PDF and can too be expressed in terms of a Meijer G-function

$$\mathbf{Pr}\left[\frac{b}{\theta} \cdot \frac{W}{I^{VU}} \leq \gamma_n\right] = \frac{G_{1\,3}^{2\,1}\left(\begin{smallmatrix}1\\ m,a,0\end{smallmatrix}\middle|\gamma_n\right)}{\Gamma(m)\Gamma(a)} \tag{5.8}$$

where $G_{1\,3}^{2\,1}\left(\begin{smallmatrix}1\\ m,a,0\end{smallmatrix}\middle|\gamma_n\right) = \frac{\Gamma(a-m)\gamma_n^m}{m} {}_1F_2(m; m+1-a, m+1; \gamma_n) + \frac{\Gamma(m-a)\gamma_n^a}{a} {}_1F_2(a; a+1-m, a+1; \gamma_n)$. Equation (5.8) can be used as the CDF of the SIR distribution by properly shifting the axis $\mathbf{Pr}\left[\frac{b}{\theta} \cdot \frac{W}{I^{VU}} \leq \gamma_n\right] = \mathbf{Pr}\left[\frac{W}{I^{VU}} \leq \frac{\theta}{b}\gamma_n\right] = \mathbf{Pr}\left[\frac{W}{I^{VU}} \leq \gamma\right]$. The mean SIR is underestimated by 2.5 dB, but the Meijer G-function is accurate in the lower tail (see Figure 5.4). In-car communication can coexist with the spectrum of indoor femtocell, while the mounted roof-top antennas generate an unacceptably high interference level at the femtocell.

5.5 Discussion

In this chapter, we discussed coexistence between indoor small-cells and vehicular communication. We developed a model useful for assessing the outage probability at the indoor femtocell due to the interference generated from vehicle communications in an ultra-dense urban scenario. We analyzed two relevant spectrum sharing scenarios and conducted the outage probability analysis in both: (i) communication from mounted antennas on the roof of the vehicles to the infrastructure network utilizes the same spectrum with indoor femtocells, and (ii) in-vehicle communication utilizes the same spectrum along with indoor femtocells while vehicle-to-infrastructure communication is allocated at a different spectrum. With mounted antennas on the top of the vehicles the outage probability becomes prohibitively high given that the density of vehicular transmissions is high too. On the other hand, with in-vehicle BSs, the isolation due to the vehicle shell and the possibility to use lower power levels inside the vehicle make it possible to maintain a low outage probability at the femtocell even for a high car density.

Note that for the analytic treatment of interference distribution in the stochastic geometry approach, our proposed model is simplified in the pathloss model and deployment model aspects. Compared to a single slope pathloss model, dual-slope models have been shown to more closely match empirical results and to have significantly different characteristics in dense networks [125, 126]. Such models use different pathloss exponents for LOS and NLOS links. Our dual-slope model is simpler, with a fixed pathloss exponent α for the NLOS link, than the UMi model in the Manhattan grid layout [121] where the pathloss exponent and attenuation constant are dependent on the LOS and NLOS link distances. The relatively simple form allows to rapidly evaluate the impact of vehicular transmissions with few input environmental parameters. Note also that, when a transmitter and receiver are located on parallel streets, more accurate interference distribution can be modeled by considering the signal components propagating through the street canyons which must turn at two intersections, namely the 2-turn NLOS pathloss model [127].

Vehicles are assumed to be distributed along a street according to a one-dimensional PPP. As shown in equation (5.4), the independent property [122] of the PPPs enables us to factorize the outage probability into separate factors for the interference contribution from each street. We can

add additional parallel lanes on the same street, but separated by a fixed distance. Note that from the practical point of view, a homogeneous PPP may not be realistic [128], since it does not capture reduced vehicle speed near the intersection in the Manhattan topology, and more sophisticated models may be required for in-homogeneous situations. In such a case, equation (5.5i) can be generalized by allowing λ_j^{vu} to be a function of the distance r, e.g., $\lambda_j^{vu}(r)$. To maintain a certain in-homogeneity of vehicles, we may further employ some random mobility models [129,130]. Also, the locations of the vehicles could be correlated according to spectrum access scheduling, i.e., vehicles with a CSMA-type MAC [131].

6. Summary and future work

6.1 Summary and conclusions

A promising solution to inefficient spectrum utilization and spectrum scarcity problem is shared use of spectrum. In this thesis, we have focused on the shared use of licensed spectrum introducing controlled interference and ensuring performance reliability to entities operating in the shared spectrum. Different spectrum sharing options in terms of spectrum access priority, technology and deployment scenario are considered. Irrespective of sharing options, the sharing entities need to somehow deal with extra interference which is one of the main parameters limiting spectral efficiency and performance gains. Thus, the main challenge in a shared use of spectrum is to manage/control the extra interference in a low-complex manner, supporting different technologies in different deployments: i) database-assisted secondary spectrum access in the TV band and ii) co-primary shared access in the cellular band.

One approach to secondary use of spectrum is to allow secondary systems to access spectrum resources that have been allocated to a primary system, under the obligation that the secondary usage does not harmfully interfere with the primary service. In addition, self-interference within the secondary system needs also to be taken into account, as in LSA mode. In this thesis, database-controlled secondary spectrum access is considered. The TV spectrum is utilized by a licensed secondary system outside of TV coverage, using the geolocation database which includes some information such as the list of available channels and operational rules for secondary access, and allocates some operational parameters to the secondary system.

We consider transmit power and CS threshold as tuning parameters.

Given the available margin, the sum rate utilities are maximized for the power allocation algorithm. Under secondary cellular converge constraints, we illustrate that the optimal power density allocation tends to be uniform. The uniform approximation reduces the amount of computations, making it possible to assess cellular capacity on a national level.

The CS threshold can be used as a common parameter for exploiting the TV spectrum more efficiently with the TV protection requirements. The parameter can be adjusted to set the maximum allowable number of active secondary nodes with the CSMA-type MAC, which limits the cross-tier interference in the TV system, and the spatial separation among the active nodes, which avoids strong self-interference in the secondary system in LSA mode. However, it is difficult to identify a common parameter due to the existence of borders and protection regions. This difficulty is resolved by a low complexity method where given the maximum density of users in finite deployment, the CS range is set and is mapped to a CS threshold.

For the co-primary shared access, we consider two different operational levels; spectrum sharing i) between two small-cells belonging to different operators, and ii) between two users belonging to different operators. The cell-level operation is about outdoor moving cells coexisting with indoor femtocell in a Manhattan street deployment. We develop a low-complexity and accurate model to capture cross-tier interference statistic and performance at the femtocell by using one-dimensional PPP. Through the proposed model, we study how the density of vehicles, the uplink transmit power level and the vehicle isolation impact the outage probability at the femtocell. We argue that for mounted roof-top antennas frequency planning between street microcells and indoor femtocells could be an option for performance enhancement, while in-vehicle and femtocell communication can coexist in the same spectrum.

The user level operation for spectrum sharing is about proximity-based short-range direct links between two end devices subscribed to different operators. We propose a mechanism for interference control and spectrum allocation for inter-operator D2D communication. One issue is about the cross-tier interference among cellular link, intra-operator D2D link, and inter-operator D2D link, which requires large amount of signaling overhead. Since operators might not be willing to reveal proprietary information, D2D overlay mode is a feasible solution for the inter-operator D2D links. In such an overlay approach, there is no cross-tier interference

among cellular and D2D links. However, the cellular spectrum might be used inefficiently. One way to improve spectrum utilization is to use proper mode selection which controls the amount of self-interference in associated D2D overlay mode in a distributed manner eliminating the communication signaling overhead between D2D users and their home BSs, based on the spectrum usage activity captured by the self-interference model.

For such inter-operator direct links, associated operators jointly use a part of their licensed spectrum. At the same time they become competitor to each other in making an offer for their contributions to a shared band. For this purpose, we use a non-cooperative game approach where participating operators reach a consensus with a proposed iterative algorithm. Using the proposed spectrum sharing solution, all operators experience significant performance gains as compared to no spectrum sharing, with low computational complexity and signaling overhead.

6.2 Future work

In this thesis, we studied the problem of modeling interference in different deployment scenarios under some assumptions leading to tractable closed-form expressions and thus, enabling an understanding of the effects of the fundamental design parameters on system behavior. One straightforward extension is to relax the assumptions and investigate how the proposed solutions may behave.

We take the fundamental assumption of the optimistic fading effect, two-dimensional deployment scenarios, one antenna per node, and frequency bands below 6 GHz. We did not take into account the combined effect of large-scale fading and small-scale fading for simplicity. We only a consider co-channel model with Lognormal fading in the TV band, and Nakagami-m and Rayleigh fading in the cellular band, since each assumption allows for performance characterization. As a future work, more generalized models for accuracy and analytical tractability are needed. With the recent release of a three-dimensional channel model [132], 3GPP has made a clear statement for the future of wireless network modeling such as beam-forming. A considerable effort should be directed towards augmenting the existing models by a third dimension [133]. Moreover, the models in this thesis only enable to account for a SISO system. Since future wireless cellular system will heavily rely on MIMO transmis-

sions [132], their support also yields an important topic for further work. Also, investigating the interplay between D2D communications and massive MIMO in other higher frequency bands, such as the mmWave, will be an interesting future direction. In mmWave systems we need directivity gain to compensate for severe channel attenuation. This directionality, however, promises a significant gain in D2D communications due to a substantially lower amount of multiuser interference in mmWave networks. Nevertheless, uncoordinated transmission in an unlicensed frequency band requires interference management.

We employed MPP type II as a repulsive point process for a CSMA-type MAC, in order to consider performance degradation by nearby transmission, i) in a secondary system for LSA and ii) in D2D communication with distributed mode selection for CSA, based on the assumption of CS range HCD δ, larger than the useful link distance $\delta > r_d$. This is mainly due to a hidden node problem issue; however, the assumption is reasonable in our proposed method due to i) in a secondary system, the doubled HCD 2δ which is originally proposed as a simple but loose upper bound for the number of points generated from a MPP type III [48], and ii) also, in D2D communication, a short useful direct link distance between the D2D pair based on proximity-based service communication. Nevertheless, still an accurate and more sophisticated interference model for a more general case is needed to reflect upon not only the hidden node problem with an RTS/CTS handshake [134] but also the exposed node problem. In addition, it will be necessary to mitigate the underestimation problem of the MPP type II not only under the relatively low density of the parent PPP [135] but also in more general high density cases.

References

[1] K. Harrison, S. M. Mishra, and A. Sahai, "How much white-space capacity is there?," in *Proc. IEEE Symposium on New Frontiers in Dynamic Spectrum*, pp. 1–10, 2010.

[2] C. Cordeiro, K. Challapali, and M. Ghosh, "Cognitive PHY and MAC layers for dynamic spectrum access and sharing of TV bands," in *Proc. International Workshop on Technology and policy for accessing spectrum*, no. 3, 2006.

[3] European Commission, "Promoting the shared use of radio spectrum resources in the internal market," *COM 478 final*, 2012.

[4] ECC, "Licensed shared access," Tech. Rep. 205, 2013.

[5] ECC, "Broadband wireless systems usage in 2300-2400 MHz," Tech. Rep. 172, 2012.

[6] M. Matinmikko, H. Okkonen, M. Palola, S. Yrjola, P. Ahokangas, and M. Mustonen, "Spectrum sharing using licensed shared access: the concept and its workflow for LTE-advanced networks," *IEEE Wireless Communications*, vol. 21, no. 2, pp. 72–79, 2014.

[7] M. Matinmikko, M. Palola, H. Saarnisaari, M. Heikkila, J. Prokkola, T. Kippola, T. Hanninen, M. Jokinen, and S. Yrjola, "Cognitive radio trial environment: First live authorized shared access-based spectrum-sharing demonstration," *IEEE Vehicular Technology Magazine*, vol. 8, no. 3, pp. 30–37, 2013.

[8] T. Baykas, M. Tuncer, M. Kasslin, M. Cummings, H. Kang, J. Kwak, R. Paine, A. Reznik, R. Saeed, and S. J. Shellhammer, "Developing a standard for TV white space coexistence: Technical challenges and solution approaches," *IEEE Wireless Communications*, vol. 19, no. 1, pp. 10–22, 2012.

[9] K. Koufos, O. Tirkkonen, T. Rosowski, J. Kronander, T. Irnich, O. Queseth, M. Tercero, and E. al, "Future spectrum system concept," *EU-Project METIS (ICT-317669), Deliverable D5.4*, 2015.

[10] A. Apostolidis, L. Campoy, K. Chatzikokolakis, K. J. Friederichs, T. Irnich, K. Koufos, J. Kronander, J. Luo, E. Mohyeldin, P. Olmos, and T. Rosowski, "Intermediate description of the spectrum needs and usage principles," *EU-Project METIS (ICT-317669) Deliverable D5.1*, 2013.

[11] Y. Luo, L. Gao, and J. Huang, "Business modeling for TV white space networks," *IEEE Communications Magazine*, vol. 53, no. 5, pp. 82–88, 2015.

[12] M. M. Kassem and M. K. Marina, "Future wireless spectrum below 6 GHz: A UK perspective," in *Proc. IEEE Dynamic Spectrum Access Networks (DySPAN)*, pp. 59–70, 2015.

[13] GSMA, "Mobile spectrum requirements and target bands for WRC-15," *Public Policy Position*, 2015.

[14] P. Ahokangas, K. Horneman, H. Posti, M. Matinmikko, T. Hanninen, S. Yrjola, and V. Goncalves, "Defining "co-primary spectrum sharing"—A new business opportunity for MNOs?," in *Proc. IEEE International Conference on Cognitive Radio Oriented Wireless Networks and Communications (CROWNCOM)*, pp. 395–400, 2014.

[15] ECC, "Technical and operational requirements for the possible operation of cognitive radio systems in the 'White Spaces' of the frequency band 470-790 MHz," Tech. Rep. 159, 2011.

[16] FCC, "In the matter of unlicensed operation in the TV broadcast bands: Second memorandum opinion and order," Tech. Rep. 10-174, 2010.

[17] H. ElSawy, E. Hossain, and M. Haenggi, "Stochastic geometry for modeling, analysis, and design of multi-tier and cognitive cellular wireless networks: A survey," *IEEE Communications Surveys & Tutorials*, vol. 15, no. 3, pp. 996–1019, 2013.

[18] P. Cardieri, "Modeling interference in wireless ad hoc networks," *IEEE Communications Surveys & Tutorials*, vol. 12, no. 4, pp. 551–572, 2010.

[19] F. Baccelli, B. Blaszczyszyn, and P. Mühlethaler, "An aloha protocol for multihop mobile wireless networks," *IEEE Transactions on Information Theory*, vol. 52, no. 2, pp. 421–436, 2006.

[20] D. Stoyan, W. S. Kendall, J. Mecke, and L. Ruschendorf, *Stochastic geometry and its applications*, vol. 2. Wiley New York, 1987.

[21] N. Akhiezer and N. Kemmer, *The classical moment problem: and some related questions in analysis*, vol. 5. Oliver & Boyd Edinburgh, 1965.

[22] M. Denker and W. Woyczynski, *Introductory statistics and random phenomena: Uncertainty, complexity and chaotic behavior in engineering and science*. Springer Science & Business Media, 2012.

[23] L. F. Fenton, "The sum of log-normal probability distributions in scatter transmission systems," *IRE Transactions on Communications Systems*, vol. 8, no. 1, pp. 57–67, 1960.

[24] S. C. Schwartz and Y. S. Yeh, "On the distribution function and moments of power sums with Log-Normal components," *Bell System Technical Journal*, vol. 61, no. 7, pp. 1441–1462, 1982.

[25] J. Wu, N. B. Mehta, and J. Zhang, "Flexible lognormal sum approximation method," in *Proc. IEEE Global Telecommunications Conference (GLOBECOM)*, vol. 6, pp. 3413–3417, 2005.

[26] O. Bulakci, J. Hamalainen, A. B. Saleh, S. Redana, and B. Raaf, "Impact of preconditioning on the convergence of numerical co-channel interference approximations in heterogeneous networks," in *Proc. International Wireless Communications and Mobile Computing Conference (IWCMC)*, pp. 119–124, 2011.

[27] Y. Selen and J. Kronander, "Optimizing power limits for white space devices under a probability constraint on aggregated interference," in *Proc. IEEE International Symposium on Dynamic Spectrum Access Networks (DYSPAN)*, pp. 201–211, 2012.

[28] H. Q. Nguyen, F. Baccelli, and D. Kofman, "A stochastic geometry analysis of dense IEEE 802.11 networks," in *Proc. IEEE International Conference on Computer Communications (INFOCOM)*, pp. 1199–1207, 2007.

[29] M. Haenggi, "Mean interference in hard-core wireless networks," *IEEE Communications Letters*, vol. 15, no. 8, pp. 792–794, 2011.

[30] R. H. Ganti and J. G. Andrews, "A new method for computing the transmission capacity of non-poisson wireless networks," in *Proc. IEEE International Symposium on Information Theory Proceedings (ISIT)*, pp. 1693–1697, 2010.

[31] A. M. Ibrahim, T. ElBatt, and A. El-Keyi, "Coverage probability analysis for wireless networks using repulsive point processes," in *Proc. IEEE International Symposium on Personal Indoor and Mobile Radio Communications (PIMRC)*, pp. 1002–1007, 2013.

[32] A. M. Hunter, J. G. Andrews, and S. Weber, "Transmission capacity of ad hoc networks with spatial diversity," *IEEE Transactions on Wireless Communications*, vol. 7, no. 12, pp. 5058–5071, 2008.

[33] J. G. Andrews, F. Baccelli, and R. K. Ganti, "A tractable approach to coverage and rate in cellular networks," *IEEE Transactions on Communications*, vol. 59, no. 11, pp. 3122–3134, 2011.

[34] K. Ruttik, K. Koufos, and R. Jäntti, "Modeling of the secondary system's generated interference and studying of its impact on the secondary system design," *Radioengineering*, vol. 19, no. 4, pp. 488–493, 2010.

[35] A. Ghosh, J. Zhang, J. G. Andrews, and R. Muhamed, *Fundamentals of LTE*. Pearson Education, 2010.

[36] D. C. Boes, F. A. Graybill, and A. M. Mood, *Introduction to the Theory of Statistics*. McGraw-Hill, New York, NY, 1974.

[37] M. Haenggi and R. K. Ganti, *Interference in large wireless networks*. Now Publishers Inc, 2009.

[38] M. Z. Win, P. C. Pinto, and L. Shepp, "A mathematical theory of network interference and its applications," vol. 97, no. 2, pp. 205–230, 2009.

[39] E. S. Sousa and J. Silvester, "Optimum transmission ranges in a direct-sequence spread-spectrum multihop packet radio network," *IEEE Journal on Selected Areas in Communications*, vol. 8, no. 5, pp. 762–771, 1990.

[40] M. Souryal, B. Vojcic, and R. Pickholtz, "Ad hoc, multihop CDMA networks with route diversity in a rayleigh fading channel," in *Proc. IEEE Military Communications Conference*, vol. 2, pp. 1003–1007, 2001.

[41] A. Hasan and J. G. Andrews, "The guard zone in wireless ad hoc networks," *IEEE Transactions on Wireless Communications*, vol. 6, no. 3, pp. 897–906, 2007.

[42] S. Srinivasa and M. Haenggi, "Modeling interference in finite uniformly random networks," in *Proc. International Workshop on Information Theory for Sensor Networks*, pp. 1–12, 2007.

[43] C. H. D. Lima, M. Bennis, and M. Latva-aho, "Coordination mechanisms for self-organizing femtocells in two-tier coexistence scenarios," *IEEE Transactions on Wireless Communications*, vol. 11, no. 6, pp. 2212–2223, 2012.

[44] A. Ghasemi and E. S. Sousa, "Interference aggregation in spectrum-sensing cognitive wireless networks," *IEEE Journal of Selected Topics in Signal Processing*, vol. 2, no. 1, pp. 41–56, 2008.

[45] A. Rabbachin, T. Q. Quek, H. Shin, and M. Z. Win, "Cognitive network interference," *IEEE Journal on Selected Areas in Communications*, vol. 29, no. 2, pp. 480–493, 2011.

[46] M. Kountouris and N. Pappas, "Approximating the interference distribution in large wireless networks," in *Proc. International Symposium on Wireless Communications Systems (ISWCS)*, pp. 80–84, 2014.

[47] J. G. Andrews, R. K. Ganti, M. Haenggi, N. Jindal, and S. Weber, "A primer on spatial modeling and analysis in wireless networks," *IEEE Communications Magazine*, vol. 48, no. 11, pp. 156–163, 2010.

[48] J. Møller, M. L. Huber, and R. L. Wolpert, "Perfect simulation and moment properties for the Matérn type III process," *Stochastic Processes and their Applications*, vol. 120, no. 11, pp. 2142–2158, 2010.

[49] A. Busson and G. Chelius, "Point processes for interference modeling in CSMA/CA ad-hoc networks," in *Proc. ACM symposium on Performance evaluation of wireless ad hoc, sensor, and ubiquitous networks*, pp. 33–40, 2009.

[50] Z. Chen, C. X. Wang, X. Hong, J. S. Thompson, S. Vorobyov, X. Ge, H. Xiao, and F. Zhao, "Aggregate interference modeling in cognitive radio networks with power and contention control," *IEEE Transactions on Communications*, vol. 60, no. 2, pp. 456–468, 2012.

[51] FCC, "In the matter of unlicensed operation in the TV broadcast bands: Third memorandum opinion and order," Tech. Rep. 12-36, 2012.

[52] ECC, "Technical and operational requirements for the operation of white space devices under geo-location approach," Tech. Rep. 186, 2013.

[53] OFCOM, "Regulatory requirements for white space device in the UHF TV band," tech. rep., 2012.

[54] M. Caleffi and A. S. Cacciapuoti, “Database access strategy for TV white space cognitive radio networks,” in *Proc. IEEE International Conference on Sensing, Communication, and Networking (SECON) Workshops*, pp. 34–38, 2014.

[55] K. Koufos, “Spectrum access in white spaces using spectrum sensing and geolocation databases,” *Dissertation, Aalto University*, 2013.

[56] R. Jäntti, J. Kerttula, K. Koufos, and K. Ruttik, “Aggregate interference with FCC and ECC white space usage rules: case study in Finland,” in *Proc. IEEE Symposium on New Frontiers in Dynamic Spectrum Access Networks (DySPAN)*, pp. 599–602, 2011.

[57] WLAN Working Group, “IEEE 802.11 af: Wireless RAN Medium Access Control (MAC) and Physical Layer (PHY) specifications amendment 5: TV white spaces operation,” 2013.

[58] ECMA-392, “MAC and PHY for Operation in TV white space,” 2012.

[59] U. H. Reimers, “DVB-the family of interantional standards for digital video broadcasting,” vol. 94, no. 1, pp. 173–182, 2006.

[60] K. Ruttik, “Secondary spectrum usage in TV white space,” *Dissertation, Aalto University*, 2011.

[61] K. Koufos, K. Ruttik, and R. Jäntti, “Controlling the interference from multiple secondary systems at the TV cell border,” in *Proc. IEEE International Symposium on Personal Indoor and Mobile Radio Communications (PIMRC)*, pp. 645–649, 2011.

[62] E. D. Anese, S. J. Kim, G. B. Giannakis, and S. Pupolin, “Power allocation for cognitive radio networks under channel uncertainty,” in *Proc. IEEE International Conference on Communications (ICC)*, pp. 1–6, 2011.

[63] K. Koufos and R. Jäntti, “Proportional fair power allocation for secondary transmitters in the TV white space,” *Journal of Electrical and Computer Engineering*, vol. 2013, p. 2, 2013.

[64] T. S. Kim, H. Lim, and J. C. Hou, “Improving spatial reuse through tuning transmit power, carrier sense threshold, and data rate in multihop wireless networks,” in *Proc. International conference on Mobile computing and networking*, pp. 366–377, ACM, 2006.

[65] R. M. Corless, G. H. Gonnet, D. E. G. Hare, D. J. Jeffrey, and D. E. Knuth, “On the LambertW function,” *Advances in Computational mathematics*, vol. 5, no. 1, pp. 329–359, 1996.

[66] A. Busson, G. Chelius, and J. M. Gorce, “Interference modeling in CSMA multi-hop wireless networks,” 2009.

[67] S. Haykin, “Cognitive radio: brain-empowered wireless communications,” *IEEE Journal on Selected Areas in Communications*, vol. 23, no. 2, pp. 201–220, 2005.

[68] K. Harrison and A. Sahai, “Potential collapse of whitespaces and the prospect for a universal power rule,” in *Proc. IEEE Symposium on New Frontiers in Dynamic Spectrum Access Networks (DySPAN)*, pp. 316–327, 2011.

[69] T. Dudda and T. Irnich, "Capacity of cellular networks deployed in TV White Space," in *Proc. IEEE International Symposium on Dynamic Spectrum Access Networks (DYSPAN)*, pp. 254–265, 2012.

[70] C. Thorpe and L. Murphy, "A survey of adaptive carrier sensing mechanisms for IEEE 802.11 wireless networks," *IEEE Communications Surveys Tutorials*, vol. 16, no. 3, pp. 1266–1293, 2014.

[71] A. Busson and G. Chelius, "Capacity and interference modeling of CSMA/CA networks using SSI point processes," *Telecommunication Systems*, vol. 57, no. 1, pp. 25–39, 2014.

[72] Y. Yang, J. C. Hou, and L.-C. Kung, "Modeling the effect of transmit power and physical carrier sense in multi-hop wireless networks," in *Proc. IEEE International Conference on Computer Communications*, pp. 2331–2335, 2007.

[73] Y. Zhang, B. Li, M. Yang, Z. Yan, and X. Zuo, "Joint optimization of carrier sensing threshold and transmission rate in wireless ad hoc networks," in *Proc. International Conference on Heterogeneous Networking for Quality, Reliability, Security and Robustness*, pp. 210–215, 2015.

[74] S. Kawade and M. Nekovee, "Broadband wireless delivery using an inside-out TV white space network architecture," in *Proc. IEEE Global Telecommunications Conference (GLOBECOM)*, pp. 1–6, 2011.

[75] L. Simić, M. Petrova, and P. Mähönen, "Wi-Fi, but not on steroids: performance analysis of a Wi-Fi-like network operating in TVWS under realistic conditions," in *Proc. IEEE International Conference on Communications (ICC)*, pp. 1533–1538, 2012.

[76] B. Cho, K. Koufos, and R. Jäntti, "Performance of secondary wireless networks with contention control in TV white spaces," *Mobile Networks and Applications*, vol. 19, no. 4, pp. 467–472, 2014.

[77] 3GPP, "Feasibility study for Proximity Services (ProSe) (Release 12)," *TR 22.803*, 2013.

[78] 3GPP, "Study on architecture enhancements to support Proximity-based Services (ProSe) (Release 12)," *TR 22.803*, 2014.

[79] 3GPP, "Study on LTE Device to Device Proximity Services: Radio Aspects (Release 12)," *TR 36.843*, 2014.

[80] P. Mach, Z. Becvar, and T. Vanek, "In-band device-to-device communication in OFDMA cellular networks: A survey and challenges," *IEEE Communications Surveys & Tutorials*, vol. 17, no. 4, pp. 1885–1922, 2015.

[81] 3GPP, "Study on architecture enhancements to support Proximity Services (Release 12)," *TR 23.703*, 2014.

[82] 3GPP, "Study on Radio Access Network (RAN) sharing enhancements (Release 12)," *TR 22.852*, 2013.

[83] 3GPP, "Study on Radio Access Network (RAN) sharing enhancements (Release 13)," *TR 22.852*, 2014.

[84] C. H. Yu, O. Tirkkonen, K. Doppler, and C. Ribeiro, "On the performance of device-to-device underlay communication with simple power control," in *Proc. IEEE Vehicular Technology Conference (VTC)*, pp. 1–5, 2009.

[85] J. Pekka, C. H. YU, R. Cassio, W. Carl, H. Klaus, T. Olav, and K. Visa, "Device-to-device communication underlaying cellular communications systems," *International Journal of Communications, Network and System Sciences*, vol. 2, p. 169, 2009.

[86] K. Doppler, M. Rinne, C. Wijting, C. B. Ribeiro, and K. Hugl, "Device-to-device communication as an underlay to LTE-advanced networks," *IEEE Communications Magazine*, vol. 47, no. 12, pp. 42–49, 2009.

[87] K. Doppler, C. H. Yu, C. B. Ribeiro, and P. Jänis, "Mode selection for device-to-device communication underlaying an LTE-advanced network," in *Proc. IEEE Wireless Communications and Networking Conference (WCNC)*, pp. 1–6, 2010.

[88] S. Hakola, T. Chen, J. Lehtomäki, and T. Koskela, "Device-to-device (D2D) communication in cellular network-performance analysis of optimum and practical communication mode selection," in *Proc. IEEE Wireless Communications and Networking Conference (WCNC)*, pp. 1–6, 2010.

[89] G. Fodor, E. Dahlman, G. Mildh, S. Parkvall, N. Reider, G. Miklós, and Z. Turányi, "Design aspects of network assisted device-to-device communications," *IEEE Communications Magazine*, vol. 50, no. 3, pp. 170–177, 2012.

[90] S. Shalmashi, G. Miao, and S. B. Slimane, "Interference management for multiple device-to-device communications underlaying cellular networks," in *Proc. IEEE Personal Indoor and Mobile Radio Communications (PIMRC)*, pp. 223–227, 2013.

[91] R. Zhang, X. Cheng, L. Yang, and B. Jiao, "Interference-aware graph based resource sharing for device-to-device communications underlaying cellular networks," in *Proc. IEEE Wireless Communications and Networking Conference (WCNC)*, pp. 140–145, 2013.

[92] S. Stefanatos, A. Gotsis, and A. Alexiou, "Analytical assessment of coordinated overlay D2D communications," in *Proc. European Wireless Conference*, pp. 1–6, 2014.

[93] V. V. Phan, L. Yu, K. Horneman, and S. J. Hakola, "D2D communications considering different network operators," *US Patent 12/763,454*, 2010.

[94] A. V. Pais and L. Jorguseski, "Multi-operator device-to-device multicast or broadcast communication," *US Patent PCT/EP2013/078064*, 2014.

[95] X. Lin, J. G. Andrews, and A. Ghosh, "Spectrum sharing for device-to-device communication in cellular networks," *IEEE Transactions on Wireless Communications*, vol. 13, no. 12, pp. 6727–6740, 2014.

[96] H. ElSawy, E. Hossain, and M. S. Alouini, "Analytical modeling of mode selection and power control for underlay D2D communication in cellular networks," *IEEE Transactions on Communications*, vol. 62, no. 11, pp. 4147–4161, 2014.

[97] C. H. Yu, O. Tirkkonen, K. Doppler, and C. Ribeiro, "Power optimization of device-to-device communication underlaying cellular communication," in *Proc. IEEE International Conference on Communications (ICC)*, pp. 1–5, 2009.

[98] C. H. Yu, K. Doppler, C. B. Ribeiro, and O. Tirkkonen, "Resource sharing optimization for device-to-device communication underlaying cellular networks," *IEEE Transaction on Wireless Communications*, vol. 10, no. 8, pp. 2752–2763, 2011.

[99] M. S. Klamkin and D. J. Newman, "Extensions of the Weierstrass product inequalities," *Mathematics Magazine*, vol. 43, no. 3, pp. 137–141, 1970.

[100] H. Moulin, *Game theory for the social sciences*. NYU press, 1986.

[101] H. Moulin, *On the uniqueness and stability of Nash equilibrium in noncooperative games*. No. 130, North-Holland Publishing Company, 1980.

[102] P. Dubey, "Inefficiency of Nash equilibria," *Mathematics of Operations Research*, vol. 11, no. 1, pp. 1–8, 1986.

[103] G. Scutari, D. P. Palomar, and S. Barbarossa, "Optimal linear precoding strategies for wideband noncooperative systems based on game theory—Part I: Nash equilibria," *IEEE Transactions on Signal Processing*, vol. 56, no. 3, pp. 1230–1249, 2008.

[104] E. Altman and T. Başar, "Multiuser rate-based flow control," *IEEE Transactions on Communications*, vol. 46, no. 7, pp. 940–949, 1998.

[105] N. Bhushan, J. Li, D. Malladi, R. Gilmore, D. Brenner, A. Damnjanovic, R. Sukhavasi, C. Patel, and S. Geirhofer, "Network densification: the dominant theme for wireless evolution into 5G," *IEEE Communications Magazine*, vol. 52, no. 2, pp. 82–89, 2014.

[106] P. Popovski, V. Braun, G. Mange, P. Fertl, D. Gozalvez-Serrano, N. Bayer, H. Droste, A. Roos, G. Zimmermann, M. Fallgren, and A. Höglund, "Initial report on horizontal topics, first results and 5G system concept," *EU-Project METIS (ICT-317669), Deliverable D6.2*, 2014.

[107] J. Gozálvez, M. Sepulcre, and R. Bauza, "IEEE 802.11p vehicle to infrastructure communications in urban environments," *IEEE Communications Magazine*, vol. 50, no. 5, pp. 176–183, 2012.

[108] E. Tanghe, W. Joseph, L. Verloock, and L. Martens, "Evaluation of vehicle penetration loss at wireless communication frequencies," *IEEE Transactions on Vehicular Technology*, vol. 57, no. 4, pp. 2036–2041, 2008.

[109] R. Schneiderman, "Car makers see opportunities in infotainment, driver-assistance systems [special reports]," *IEEE Signal Processing Magazine*, vol. 1, no. 30, pp. 11–15, 2013.

[110] 3GPP, "Technical Specification Group Radio Access Network; Mobile Relay for Evolved Universal Terrestrial Radio Access (E-UTRA)," *TR 36.836*, 2014.

[111] B. Kaufman, J. Lilleberg, and B. Aazhang, "Femtocell architectures with spectrum sharing for cellular radio networks," *International Journal of Advances in Engineering Sciences and Applied Mathematics*, vol. 5, no. 1, pp. 66–75, 2013.

[112] V. Chandrasekhar, J. G. Andrews, T. Muharemovic, Z. Shen, and A. Gatherer, "Power control in two-tier femtocell networks," *IEEE Transactions on Wireless Communications*, vol. 8, no. 8, pp. 4316–4328, 2009.

[113] S. Wang, C. Turyagyenda, and T. O'Farrell, "Energy efficiency and spectral efficiency trade-off of a novel interference avoidance approach for LTE-femtocell networks," in *Proc. IEEE Vehicular Technology Conference (VTC)*, pp. 1–5, 2012.

[114] V. V. Phan, K. Horneman, L. Yu, and J. Vihriala, "Providing enhanced cellular coverage in public transportation with smart relay systems," in *Proc. IEEE Vehicular Networking Conference (VNC)*, pp. 301–308, 2010.

[115] P. Mach and Z. Becvar, "Path selection in WiMAX networks with mobile relay stations," in *Proc. International Conference on Networks*, 2011.

[116] Y. Sui, J. Vihriala, A. Papadogiannis, M. Sternad, W. Yang, and T. Svensson, "Moving cells: a promising solution to boost performance for vehicular users," *IEEE Communications Magazine*, vol. 51, no. 6, pp. 62–68, 2013.

[117] Y. Sui, I. Guvenc, and T. Svensson, "Interference management for moving networks in ultra-dense urban scenarios," *EURASIP Journal on Wireless Communications and Networking*, vol. 2015, no. 1, pp. 1–32, 2015.

[118] P. Agyapong, V. Braun, M. Fallgren, A. Gouraud, M. Hessler, S. Jeux, A. Klein, J. Lianghai, D. Martin-Sacristan, M. Maternia, and M. Moisio, "Simulation guidelines," *EU-Project METIS (ICT-317669), Deliverable D6.1*, 2013.

[119] E. Steinmetz, M. Wildemeersch, T. Quek, and H. Wymeersch, "A stochastic geometry model for vehicular communication near intersections," in *Proc. IEEE Global Communications (GLOBECOM) Workshops*, 2015.

[120] J. B. Andersen, T. S. Rappaport, and S. Yoshida, "Propagation measurements and models for wireless communications channels," *IEEE Communications Magazine*, vol. 33, no. 1, pp. 42–49, 1995.

[121] M. Series, "Guidelines for evaluation of radio interface technologies for IMT-advanced," *Report ITU*, pp. 2135–1, 2009.

[122] M. Dale, *The algebra of random variables*. Springer, 1979.

[123] D. Zwillinger, *Table of integrals, series, and products*. Elsevier, 2014.

[124] M. D. Springer and W. E. Thompson, "The distribution of products of Beta, Gamma and Gaussian random variables," *SIAM Journal on Applied Mathematics*, vol. 18, no. 4, pp. 721–737, 1970.

[125] V. Erceg, S. Ghassemzadeh, M. Taylor, L. Dong, and D. L. Schilling, "Urban/suburban out-of-sight propagation modeling," *IEEE Communications Magazine*, vol. 30, no. 6, pp. 56–61, 1992.

[126] Z. Xinchen and J. G. Andrews, "Downlink cellular network analysis with multi-slope path loss models," *IEEE Transactions on Communications*, vol. 63, no. 5, pp. 1881–1894, 2015.

[127] J. S. Lu, H. L. Bertoni, K. A. Remley, W. F. Young, and J. Ladbury, "Site-specific models of the received power for radio communication in urban street canyons," *IEEE Transactions on Antennas and Propagation*, vol. 62, no. 4, pp. 2192–2200, 2014.

[128] Y. Jeong, J. W. Chong, H. Shin, and M. Z. Win, "Intervehicle communication: Cox-Fox modeling," *IEEE Journal on Selected Areas in Communications*, vol. 31, no. 9, pp. 418–433, 2013.

[129] D. B. Johnson and D. A. Maltz, "Dynamic source routing in ad hoc wireless networks," in *Mobile computing*, pp. 153–181, Springer, 1996.

[130] C. Bettstetter, "Mobility modeling in wireless networks: categorization, smooth movement, and border effects," *SIGMOBILE Mobile Computing and Communications Review*, vol. 5, no. 3, pp. 55–66, 2001.

[131] M. J. Farooq, H. ElSawy, and M.-S. Alouini, "Modeling inter-vehicle communication in multi-lane highways: A stochastic geometry approach," in *Proc. IEEE Vehicular Technology Conference (VTC)*, 2015.

[132] 3GPP, "Study on 3D channel model for LTE (Release 12)," *TR 36.873*, 2015.

[133] J. Riihijärvi, P. Mähönen, and M. Petrova, "What will interference be like in 5G HetNets?," *Physical Communication*, 2015.

[134] Y. Zhong, W. Zhang, and M. Haenggi, "Stochastic analysis of the mean interference for the RTS/CTS mechanism," in *Proc. IEEE International Conference on Communications (ICC)*, pp. 1996–2001, 2014.

[135] H. ElSawy, E. Hossain, and S. Camorlinga, "Characterizing random CSMA wireless networks: A stochastic geometry approach," in *Proc. IEEE International Conference on Communications (ICC)*, pp. 5000–5004, 2012.

Aalto-DD 125/2016

ISBN 978-952-60-6887-9 (printed)
ISBN 978-952-60-6888-6 (pdf)
ISSN-L 1799-4934
ISSN 1799-4934 (printed)
ISSN 1799-4942 (pdf)

Aalto University
School of Electrical Engineering
Department of Communications and Networking
www.aalto.fi

BUSINESS +
ECONOMY

ART +
DESIGN +
ARCHITECTURE

SCIENCE +
TECHNOLOGY

CROSSOVER

DOCTORAL
DISSERTATIONS